Forest-atmosphere exchange of reactive nitrogen in a remote region – Part II: Modeling annual budgets

Pascal Wintjen[1], Frederik Schrader[1], Martijn Schaap[2,3], Burkhard Beudert[4], Richard Kranenburg[2], and Christian Brümmer[1]

[1]Thünen Institute of Climate-Smart Agriculture, Bundesallee 68, 38116 Braunschweig, Germany
[2]TNO, Climate Air and Sustainability, Utrecht, 3584 CB, The Netherlands
[3]Institute of Meteorology, Freie Universität Berlin, 12165 Berlin, Germany
[4]Bavarian Forest National Park, 94481, Grafenau, Germany

Correspondence to: Pascal Wintjen (pascal.wintjen@thuenen.de)

Abstract. To monitor the effect of current nitrogen emissions and mitigation strategies, total (wet+dry) atmospheric nitrogen deposition to forests is commonly estimated using chemical transport models or canopy budget models in combination with throughfall measurements. Since flux measurements of reactive nitrogen (N_r) compounds are scarce, dry deposition process descriptions as well as the calculated flux estimates and annual budgets are subject to considerable uncertainties. In this study, we compared four different approaches to quantify annual dry deposition budgets of total reactive nitrogen (ΣN_r) at a mixed forest site situated in the Bavarian Forest National Park, Germany. Dry deposition budgets were quantified based on (I) 2.5 years of eddy-covariance flux measurements with the Total Reactive Atmospheric Nitrogen Converter (TRANC), (II) an in-situ application of the bidirectional inferential resistance scheme DEPAC (Deposition of Acidifying Compounds), here called DEPAC-1D, (III) a simulation with the chemical transport model LOTOS-EUROS (LOng Term Ozone Simulation – EURopean Operational Smog) v2.0 using DEPAC as dry deposition module, and (IV) a canopy budget technique (CBT).

Averaged annual ΣN_r dry deposition estimates determined from TRANC measurements were 4.7±0.2 and 4.3±0.4 kg N ha^{-1} a^{-1} depending on the gap-filling approach. DEPAC-1D modeled dry deposition, using concentrations and meteorological drivers measured at the site, was 5.8±0.1 kg N ha^{-1} a^{-1}. In comparison to TRANC fluxes, DEPAC-1D estimates were systematically higher during summer, and in close agreement in winter. Modeled ΣN_r deposition velocities (v_d) of DEPAC-1D were found to increase with lower temperatures, higher relative humidity, and in the presence of wet leaf surfaces, in particular from May to September. This observation was in contradiction to TRANC-observed fluxes. LOTOS-EUROS modeled annual dry deposition was 6.5±0.3 kg N ha^{-1} a^{-1} for the site-specific weighting of land-use classes within the site's grid cell. LOTOS-EUROS showed substantial discrepancies to measured ΣN_r deposition during spring and autumn, which was related to an overestimation of ammonia (NH_3) concentrations by a factor of two to three compared to measured values as a consequence of a mismatch between gridded input NH_3 emissions and the site's actual, rather low, pollution climate. According to LOTOS-EUROS predictions, ammonia contributed most to modeled input ΣN_r concentrations, whereas measurements showed NO_x as the prevailing compound in ΣN_r concentrations. Annual deposition estimates from measurements and modeling were in the range of minimum and maximum estimates determined from CBT being at 3.8±0.5 and 6.7±0.3 kg N ha^{-1} a^{-1}, respectively. By adding locally measured wet-only deposition, we estimated an annual total nitrogen deposition input between 11.5 and 14.8 kg N ha^{-1} a^{-1}, which is within the critical load ranges proposed for deciduous and coniferous forests.

1 Introduction

In the last century, global nitrogen emissions have increased significantly due to anthropogenic activities (Fowler et al., 2013). Reactive nitrogen compounds, such as ammonia (NH_3) and nitrogen oxides (NO_x), contribute most to the emissions. Ammonia emissions originate mostly from animal husbandry and fertilizer application (Sutton et al., 2011, 2013), whereas NO_x emissions are mainly related to combustion processes in, e.g., transport and industry (Erisman et al., 2011, 2013). Although fertilizer use and the internal combustion engine are vital for world's food security and the economy, the release of these compounds into the atmosphere has a wide range of negative effects (Krupa, 2003; Galloway et al., 2003; Erisman et al., 2013). Deposition of reactive nitrogen into ecosystems has been identified as a reduction factor for biodiversity (Bobbink et al., 1998; Krupa, 2003; Galloway et al., 2003; Sutton et al., 2011). Especially ecosystems with nutrient poor soils are highly sensitive to additional nitrogen inputs resulting in a change in plant species (Damgaard et al., 2011; Paulissen et al., 2016) and species composition in forests (Dirnböck et al., 2014, 2018; Roth et al., 2022). Critical loads are used to show at which level long-term nitrogen deposition may lead to adverse impacts (Hettelingh et al., 1995). Investigations by Hettelingh et al. (2013) have shown that half of the European ecosystems receive nitrogen above the critical level. In Germany, the fraction of ecosystems with a critical load exceedance is estimated to be about 70 % (Schaap et al., 2018).

Quantitative estimation of the total nitrogen deposition is needed to assess exceedances of critical loads and to develop successful mitigation strategies. Although wet deposition is relatively straightforward to measure, the accurate quantification of dry N deposition remains a challenge. Recent progress in fast and robust measurement techniques allowed to investigate the temporal dynamics in concentrations and dry deposition fluxes (using the eddy-covariance (EC) approach) for total reactive nitrogen (ΣN_r) (Marx et al., 2012; Ammann et al., 2012; Brümmer et al., 2013, 2022; Zöll et al., 2019; Ammann et al., 2019; Wintjen et al., 2020, 2022) and its individual compounds, e.g. for NH_3 (Whitehead et al., 2008; Ferrara et al., 2012, 2021; Zöll et al., 2016; Moravek et al., 2020). For ΣN_r, the total reactive atmospheric nitrogen converter (TRANC) (Marx et al., 2012) coupled to a chemiluminescence detector (CLD) has shown its suitability for flux measurements in various field applications (see references for ΣN_r above). Despite the recent progress, the number and temporal coverage of available datasets remains small. As these in-situ measurements are only valid for the ecosystem where the specific observations took place, a large-scale assessment based on observations alone is not feasible without a dense observation network.

Chemical transport models (CTMs) are used to assess nitrogen deposition over large regions. For Germany, the CTM LOTOS-EUROS (Wichink Kruit et al., 2012; Manders et al., 2017; van der Graaf et al., 2020) is applied for the mapping of nitrogen deposition fluxes across the country. LOTOS-EUROS predicts the dry deposition of various N_r compounds, namely nitrogen dioxide (NO_2), nitric oxide (NO), nitric acid (HNO_3), ammonia (NH_3), and particulate ammonium (NH_4^+) and nitrate (NO_3^-), in each grid cell by utilizing meteorological data from the European Centre for Medium Range Weather Forecasts (ECMWF), modeled concentrations of the mentioned compounds based on their emission sources and chemical processing, as well as information about the land-use distribution within each grid cell. The deposition module DEPAC (Deposition of Acidifying Compounds) is applied for calculating dry deposition velocities of those compounds (Erisman et al., 1994). DEPAC is a dry deposition inferential scheme featuring bidirectional NH_3 exchange (van Zanten et al., 2010; Wichink Kruit et al., 2012), which is also implemented in the Operational Priority Substance (OPS) model (van Jaarsveld, 2004; Sauter et al., 2020). DEPAC can be used as stand-alone model for estimating dry deposition of N_r compounds. For site-based modeling with DEPAC, decoupled from a CTM and henceforth called DEPAC-1D, only measurements of common micrometeorological variables and concentrations of the individual N_r compounds are needed. In the past, deposition estimates have often been obtained through such an inferential modeling approach (Flechard et al., 2011, 2020; Li et al., 2016; Schwede et al., 2011).

To evaluate modeled annual total dry deposition and seasonal patterns in modeled fluxes and deposition velocities, a careful comparative analysis to flux measurements may provide feedback on the representativeness of the input data and the bidirectional parametrizations (Wichink Kruit et al., 2010; Wichink Kruit et al., 2017). Wintjen et al. (2022) presented and analyzed novel flux measurements of ΣN_r and several subcomponents focusing on temporal dynamics above a remote, mixed forest site spanning a 2.5-year period. This dataset provides a unique opportunity for the evaluation of different approaches to quantify dry deposition fluxes. Such comparisons with novel measurement techniques are sparse and only available from few field campaigns (Ammann et al., 2012; Brümmer et al., 2013, 2022; Zöll et al., 2019). Since the adoption of the Geneva Convention on Long-Range Transboundary Air Pollution (CLRTAP) in 1979, throughfall measurements has been carried out at many sites of the International Co-operative Programmes on Assessment and Monitoring of Air Pollution Effects on Forests (ICP Forests, www.icp-forests.net, last access: 14 March 2022) and forested catchments (ICP Integrated Monitoring, http://www.syke.fi/nature/icpim, last access: 14 March 2022) according to standardized protocols. Using the so-called canopy budget technique (CBT), throughfall measurements also allow to give an estimate of the annual nitrogen dry deposition (Draaijers and Erisman, 1995; de Vries et al., 2003).

In this study, we provide a comparison of four independent methods for estimating nitrogen dry deposition for a remote mixed forest site in the Bavarian Forest National Park. The comparison is made for a 2.5 year period for which novel flux measurements were available (see companion paper Wintjen et al., 2022). The aim of this measurement campaign covering the time frame from January 2016 to June 2018 was to quantify background concentration and deposition levels as well as their temporal dynamics for further improvements in modeling nitrogen deposition that may be used for further defining environmental protection guidelines. Therefore, (1) we present modeled concentrations, deposition velocities, and fluxes of ΣN_r and compare them to measurements of the same compounds , (2) discuss the influence of micrometeorological parameters on modeled deposition velocities and the impact of measured and modeled input parameters on modeled fluxes , (3) compare annual N_r budgets of LOTOS-EUROS with DEPAC-1D, flux measurements, and nitrogen deposition estimates based on CBT and reviewing them in the context of critical loads and (4) finally discuss uncertainties affecting modeled dry deposition estimates.

2 Materials and Methods

2.1 Data set description

For the comparison to modeled ΣN_r deposition fluxes, TRANC EC flux measurements described in detail in Wintjen et al. (2022) were used. These flux measurements were available at half-hourly resolution, carried out 30 m above the forest floor, and had a data coverage of 41.0 % considering the entire campaign period. Data gaps were related to violations of the EC theory and performance issues of the instruments.

For the application of DEPAC-1D, time series of micrometeorological parameters (i.e. temperature, atmospheric pressure, relative humidity, global radiation, Obukhov length (L), friction velocity (u_*)) and air pollutant concentrations (NO, NO_2, HNO_3, NH_3, pNO_3^-, pNH_4^+, and sulphur dioxide (SO_2)) are required for flux calculations. NH_3 concentrations obtained from Quantum cascade laser measurements taken at 30 m above ground, NO_2 and NO obtained from chemiluminescence measurements taken at 50 m above ground as well as micrometeorological parameters were aggregated at half-hourly resolution, whereas the remaining N_r species and an additional NH_3 determination were obtained from DELTA (DEnuder for Long-Term Atmospheric sampling, e.g., Sutton et al., 2001; Tang et al., 2009) and passive sampler (NH_3 only) measurements of the IVL type (Ferm, 1991) for on monthly basis. DELTA measurements were made at 30 m and passive sampler measurements at 10, 20, 30, 40, and 50 m above ground. Temperature and relative humidity were collected in a profile at 10,

20, 40, and 50 m above ground. Pressure and global radiation measurements were taken at 50 m. Indicators of stability and turbulence such as L and u_* were obtained from momentum flux measurements of the sonic anemometer.

120   Gaps in DEPAC-1D were related to gaps in micrometeorological input data and issues in the measurements of N_r compounds. Respective half-hourly values in the flux time series of each gas (approx. 3.4% for NH_3, HNO_3, pNH_4^+, and pNO_3^- and 9.3% for NO and NO_2) were filled with results from LOTOS-EUROS. A detailed description of the site and the instrumentation is given in Wintjen et al. (2022). For LOTOS-EUROS flux modeling, modeled input data of the European Centre for Medium range Weather Forecast (ECMWF) and the national emission inventory of Germany (Schneider et al., 2016) were used to

125   predict deposition fluxes for NO, NO_2, HNO_3, NH_3, pNO_3^-, and pNH_4^+. LOTOS-EUROS fluxes were resampled to half-hourly timestamps from the original hourly resolution and missing fluxes were linearly interpolated. For the canopy budget technique, hroughfall measurements under spruce and beech trees in close proximity to the station (Beudert et al., 2014) and bulk deposition measurements at an open site (Wintjen et al., 2022) were taken in weekly intervals and used for determination of total nitrogen dry deposition on annual basis (Sect. 2.3). An overview of all methods is given in Table 1.

130

Table 1 Overview of methods used for estimating ΣN_r dry deposition.

Method	Primary input/observation variables and temporal resolution	Primary output variables and temporal resolution
TRANC	Wind components (u,v,w), sonic temperature (T_s), and ΣN_r concentration at 10 Hz resolution	ΣN_r fluxes at half-hourly resolution, no gap-filling applied
DEPAC-1D	Measurements of micrometeorological variables at half-hourly resolution Measured NH_3, NO, NO_2 concentrations at half-hourly resolution Measured SO_2, HNO_3, NH_3, pNO_3^-, and pNH_4^+ concentrations at monthly resolution	Fluxes of NH_3, NO_2, NO, HNO_3, pNH_4^+, and pNO_3^- at continuous half-hourly resolution
TRANC (DEPAC-1D)	See above	Continuous ΣN_r fluxes at half-hourly resolution, only DEPAC-1D is used for gap-filling
TRANC (MDV+DEPAC-1D)	See above	Continuous ΣN_r fluxes at half-hourly resolution, gap-filled with a combination of MDV (window size of ±5 days) and DEPAC-1D for adding further missing fluxes
LOTOS-EUROS	Meteorological data from ECMWF weather forecasts and modeled concentrations of SO_2, NH_3, NO_2, NO, HNO_3, pNH_4^+,	Continuous fluxes of NH_3, NO_2, NO, HNO_3, pNH_4^+, and pNO_3^- at hourly resolution; fluxes were

	and pNO_3^- at hourly resolution for $7x7$ km^2 grid cell; concentrations were linearly resampled to half-hourly resolution	linearly resampled to half-hourly resolution
Canopy budget technique	Throughfall measurements from nearby spruce and beech trees and bulk deposition measurements at an open-site in weekly intervals	Dissolved inorganic nitrogen deposition (DIN) based on the exchange of NO_3^- and NH_4^+ ions on monthly basis following the approaches of Draaijers and Erisman (1995) and de Vries et al. (2003), dissolved organic nitrogen (DON) corresponds to difference of DON fluxes between throughfall and bulk deposition

To compare dry deposition estimates from modeling to TRANC measurements, we filled gaps in the TRANC flux data with results from DEPAC-1D and henceforth, called this dataset TRANC(DEPAC-1D). In a second approach, we applied the mean-diurnal-variation (MDV) method to short-term gaps analogous to Wintjen et al. (2022) and replaced remaining gaps with results from DEPAC-1D. This approach was called TRANC(MDV+DEPAC-1D). Both approaches, DEPAC-1D alone and the combination of DEPAC-1D and MDV, were able to fill all gaps in TRANC flux time series. Uncertainties of the gap-filled fluxes determined by MDV were calculated as the standard error of the mean. Cumulative uncertainties of TRANC fluxes were solely based on the uncertainty of the gap-filling and were calculated according to Eq. (3) of Wintjen et al. (2022). The error calculation scheme proposed by Brümmer et al. (2022, Eq. (1)) was applied to fluxes filled with DEPAC-1D. Flux uncertainty of those half-hourly values was given as

$$F_{\text{unc,DEPAC}-1D} = \frac{\tilde{X}}{F_{\text{DEPAC}-1D}} \; ; \; \text{with } \tilde{X} = \frac{F_{\text{unc,meas}}}{F_{\text{meas}}}$$

(1)

where $\tilde{X}$ represents the median of the ratio of the uncertainty of the measured fluxes ($F_{\text{unc,meas}}$) to their corresponding flux values (F_{meas}). The uncertainty of the measured fluxes was estimated after Finkelstein and Sims (2001). Systematic uncertainties were not accounted in the error calculation. A discussion on systematic uncertainties is given in Wintjen et al. (2022).

2.2 Modeling reactive nitrogen fluxes

2.2.1 Bidirectional resistance model DEPAC

In surface-atmosphere exchange models, fluxes are calculated by using resistance schemes. In case of gases exhibiting bidirectional exchange behavior, the flux F is defined as follows

$$F = -v_d(z-d) \cdot (\chi_a(z-d) - \chi_{\text{tot}})$$

(2)

The flux is a product of the deposition velocity (v_d) with the concentration difference between the atmospheric concentration and the compensation point of the trace gas χ_a. In DEPAC, a compensation point is only implemented for NH_3. Both, the dry deposition or exchange velocity and the atmospheric concentration, are height dependent and given for an aerodynamic

reference height ($z - d$) where z is the geometric height and d the zero-plane displacement height. The following convention is used for the fluxes: negative values represent deposition, positive values emission. Following the conductivity-resistance analogy, v_d is the inverse of the sum of the aerodynamic resistance (R_a), the quasi-laminar layer resistance (R_b), and the canopy resistance (R_c).

$$v_d = (R_a + R_b + R_c)^{-1} \tag{3}$$

DEPAC (van Zanten, et al., 2010) can be used to calculate the dry deposition of reactive nitrogen gases. R_a and R_b are required by DEPAC as input variables. Hence, the module is oriented at determining R_c for NO, NO$_2$, HNO$_3$, and NH$_3$. R_c is treated differently for each N$_r$ compound but basically as the sum of parallel resistances, which model the exchange behavior of the atmosphere and vegetation:

$$R_c^{-1} = R_w^{-1} + R_{stom}^{-1} + (R_{inc} + R_{soil})^{-1} \tag{4}$$

The stomatal resistance (R_{stom}) is calculated following Emberson et al. (2000a, b). In this scheme, stomatal conductance is determined by vegetation type dependent on maximum conductance lowered by factors controlling stomatal opening, i.e. light intensity, ambient temperature, vapor pressure deficit, and soil water content, using well known Jarvis functions (Jarvis, 1976). For NH$_3$ a stomatal compensation point (χ_{stom}) is calculated following Wichink Kruit et al. (2010, 2017). The cuticular resistance (R_w) is described by Sutton and Fowler (1993) for NH$_3$ and the corresponding cuticular compensation point based on the works of Wichink Kruit et al. (2010, 2017). For NO and NO$_2$, R_w is set considerably high to 10000 and 2000 s m^{-1}, respectively, allowing hardly any deposition on external surfaces. The in-canopy resistance (R_{inc}) is given by van Pul and Jacobs (1994), and the soil resistance (R_{soil}) is described following Erisman and van Pul (1994). In the current version of DEPAC, the soil compensation point is set to zero for all surface types. In case of HNO$_3$, a fast uptake to any surface is assumed through a low, constant R_c of 10 s m^{-1}. The total compensation point (χ_{tot}) is determined as written in van Zanten et al. (2010).

$$\chi_{tot} = \frac{R_c}{R_w} \cdot \chi_w + \frac{R_c}{R_{inc} + R_{soil}} \cdot \chi_{soil} + \frac{R_c}{R_{stom}} \cdot \chi_{stom} \tag{5}$$

For further details to the documentation of DEPAC, we refer to the publication of van Zanten et al. (2010). Following implementation in LOTOS-EUROS, the version of DEPAC used in this study differs from the one documented in van Zanten et al. (2010) in two main aspects: Firstly, the implementation of a function considering co-deposition of SO$_2$ and NH$_3$ (Wichink Kruit et al., 2017) in the non-stomatal pathway and secondly, the usage of a monthly moving NH$_3$ average concentration for determining the stomatal compensation point (Wichink Kruit et al., 2017).

2.2.2 Modeling of ΣN$_r$ deposition (LOTOS-EUROS)

LOTOS-EUROS (Manders et al., 2017) simulations were performed for the entire measurement period. For this purpose, a large-scale simulation was setup for Europe in which a second domain covering northwestern Europe at 7×7 km^2 was nested. The simulations were forced with weather data from the ECMWF and the CORINE-2012 land-use classification. For the European background simulation, the CAMS-REG European emission inventory (Kuenen et al., 2021) was used. For the inner domain the emission data for Germany were replaced by the national emission inventory. For Germany, the gridded emissions were obtained from the GrETa system (*GRETA – Gridding Emission Tool for ArcGIS v1.1*; Schneider et al., 2016). On hourly basis, the land-use specific total dry deposition was calculated in LOTOS-EUROS by applying DEPAC for NH$_3$, NO, NO$_2$, and HNO$_3$. Dry deposition of pNO$_3^-$ and pNH$_4^+$ was calculated according to Zhang et al. (2001) (see Manders-Groot et al. (2016, Sect. 5.2)). In the model, the dry deposition velocity and flux are calculated for the mid-layer height of the first model layer, which has a depth of ca. 20 m. By assuming a constant flux and using the stability parameters, the concentrations can

190 be estimated for the canopy top and the typical observation height (2.5 m above roughness length (z_0)) in air quality networks. The Corine Land Cover 2012 classification of the grid cell, in which the measurement site was located, was divided into 46.0 % seminatural vegetation, 37.2 % coniferous forest, 15.9 % deciduous forest, 0.7 % water bodies, and 0.2 % grassland. However, the actual structure of the forest stand showed 81.1 % coniferous forest and 18.9 % deciduous forest within the footprint of the flux measurements during the measurement campaign. Due to differences in the distribution of vegetation

195 types in the footprint, results from LOTOS-EUROS were calculated with the site-specific weighting of land-use classes of the flux tower's footprint. The low contribution of coniferous forest and deciduous forest within the grid cell may be related to the evaluation of older aerial photographs showing larger areas of deadwood. Finally, the dry deposition of ΣN_r was calculated as the sum of the individual N_r fluxes. A detailed documentation of LOTOS-EUROS is given in Manders-Groot et al. (2016) and Manders et al. (2017).

2.2.3 Site-based modeling of ΣN_r deposition (DEPAC-1D)

DEPAC-1D is a stand-alone version of LOTOS-EUROS' dry deposition module DEPAC using a FORTRAN90 wrapper program to accept arbitrary input datasets. DEPAC-1D used micrometeorological variables and parameters measured at the site to estimate R_c and the compensation point of NH_3. The atmospheric resistances – R_a and R_b – and the fluxes of NH_3, NO, NO_2, HNO_3, pNO_3^-, and pNH_4^+ were calculated outside DEPAC following Garland (1977) and Jensen and Hummelshøj (1995,

205 1997) with stability corrections after Webb (1970) and Paulson (1970). The deposition of particles was calculated following Zhang et al. (2001) (see also Manders-Groot et al. (2016, Sect. 5.2)) and therewith equal to LOTOS-EUROS. For the fine fraction of pNO_3^- and pNH_4^+, a mass median diameter of 0.7 μm was used. For the coarse fraction of pNO_3^-, 8 μm was taken (Manders-Groot et al. (2016, Sect. 5.2)). Note that particle deposition is strictly speaking not part of the DEPAC module and was modeled with a separate program implementing the particle deposition scheme used within LOTOS-EUROS.

210

Half-hourly gaps in the NH_3 QCL concentration time series were filled with their monthly integrated concentration value obtained from DELTA samplers. If these measurements were not available, missing values were replaced by monthly integrated results from passive sampler measurements of NH_3. During winter, the uncertainty introduced by this gap-filling approach seems to be low as suggested by Schrader et al. (2018). We did not superimpose gap-filled concentration values with

215 a diurnal pattern or used monthly averages of half-hours to fill gaps in concentration time series, since abrupt changes in the NH_3 concentration pattern, i.e. periods of low auto-correlation could not be reproduced by a synthetic diurnal cycle or monthly averages of half-hourly values. Fluxes of HNO_3, NO_3^-, and NH_4^+ solely based on monthly DELTA measurements. Gaps in time series of these compounds and SO_2 were replaced by monthly averages from adjacent years. NO and NO_2 fluxes were based on half-hourly concentration measurements. The difference in measuring height was considered in the calculation of R_a.

220 SO_2 and NH_3 concentrations from gap-filled DELTA time series were used to determine compensation points and additional deposition corrections.

Since measurements of temperature and relative humidity data were not available at the measurement height of the EC system, we took the average of measurements from 20 m and 40 m height above ground. These profile measurements started in April 2016 (Wintjen et al., 2022), and thus measurements at 50 m were used until end of March 2016. For modeling R_a, the solar

225 zenith angle, which is calculated by using celestial mechanic equations, z_0, and d are needed. We set z_0 to 2.0 m and d to 12.933 m for coniferous forest and to 11.60 m for deciduous forest, corresponding to LOTOS-EUROS defaults for these land-use classes. Leaf area index (LAI) was modeled as described by van Zanten et al. (2010). The LAI determined from the site-specific land-use class weighting ranged between 4.1 and 4.8 due to leaf growth and shedding.

230   The calculation of the dry deposition was made for NH_3, NO, NO_2, HNO_3, pNO_3^-, and pNH_4^+ with the mentioned input data on half-hourly basis. Results from DEPAC-1D were weighted with the site-specific land-use distribution within the flux measurement's footprint (81.1 % coniferous forest and 18.9 % deciduous forest).

2.3 Measuring nitrogen outflow from the canopy using the Canopy Budget Technique (CBT)

The canopy budget technique (CBT) is the most common method for estimating total (wet+dry) atmospheric deposition of

235   dissolved inorganic nitrogen (DIN_t) based on wet inorganic nitrogen fluxes of NO_3^- and NH_4^+-ions estimated from open-site precipitation (bulk deposition) and throughfall of NO_3^- and NH_4^+-ions measurements (see Staelens et al., 2008, Table 1). DIN_t was estimated on monthly basis after the CBT approach of Draaijers and Erisman (1995) and de Vries et al. (2003). The results from the two methods differed only marginally and were therefore averaged. The biological conversion of deposited inorganic nitrogen into dissolved organic nitrogen (DON) in the phyllosphere (bacteria, yeasts, and fungi) or the

240   dry deposition of atmospheric DON onto the canopy or the exudation of DON from plant tissues is not addressed in CBT. Here, it was estimated by the difference of DON fluxes between throughfall and bulk deposition, and henceforth called ΔDON. Adding ΔDON to throughfall DIN or to DIN_t reveals a frame of lower and upper estimates of total (wet+dry) nitrogen deposition (N_t) and, by subtracting DIN deposition at an open land site from these N_t, of lower and upper estimates of dry deposition (Beudert and Breit, 2014).

245

3 Results

3.1 Comparison of modeled and measured concentrations

3.1.1 High resolution concentration measurements of NH_3, NO_x, and ΣN_r

Figure 1 shows the comparison of measured half-hourly NH_3, NO_x, and ΣN_r concentrations (*cf.* Wintjen et al., 2022) to their

250   modeled concentrations of LOTOS-EUROS represented as monthly box-whisker plots. From high-resolution concentration measurements, we found average concentrations and standard deviations of 1.0 ± 0.6, 1.4 ± 1.2, and 3.1 ± 1.7 µg N m^{-3} for NH_3, NO_x, and ΣN_r for the entire campaign, respectively. Corresponding averages of LOTOS-EUROS of NH_3 and ΣN_r were higher by 0.8 and 1.9 µg N m^{-3}, whereas NO_x was slightly underestimated. Substantial mismatches in standard deviations of NH_3 and ΣN_r indicate that the variability in concentrations of NH_3 and ΣN_r was overestimated by LOTOS-EUROS. In case of

255   NH_3, largest discrepancies were observed for spring and partially for autumn. NO_x concentrations were systematically underestimated by LOTOS-EUROS in summer. During winter, difference between measured and modeled NO_x concentrations was lower than during summer time. Except for the summer, modeled half-hourly concentrations of ΣN_r were two to three times higher than the measured values. The slight seasonal differences in measured ΣN_r concentrations could not be reproduced by LOTOS-EUROS. The largest discrepancy during spring clearly correlates with the modeled NH_3 concentrations.
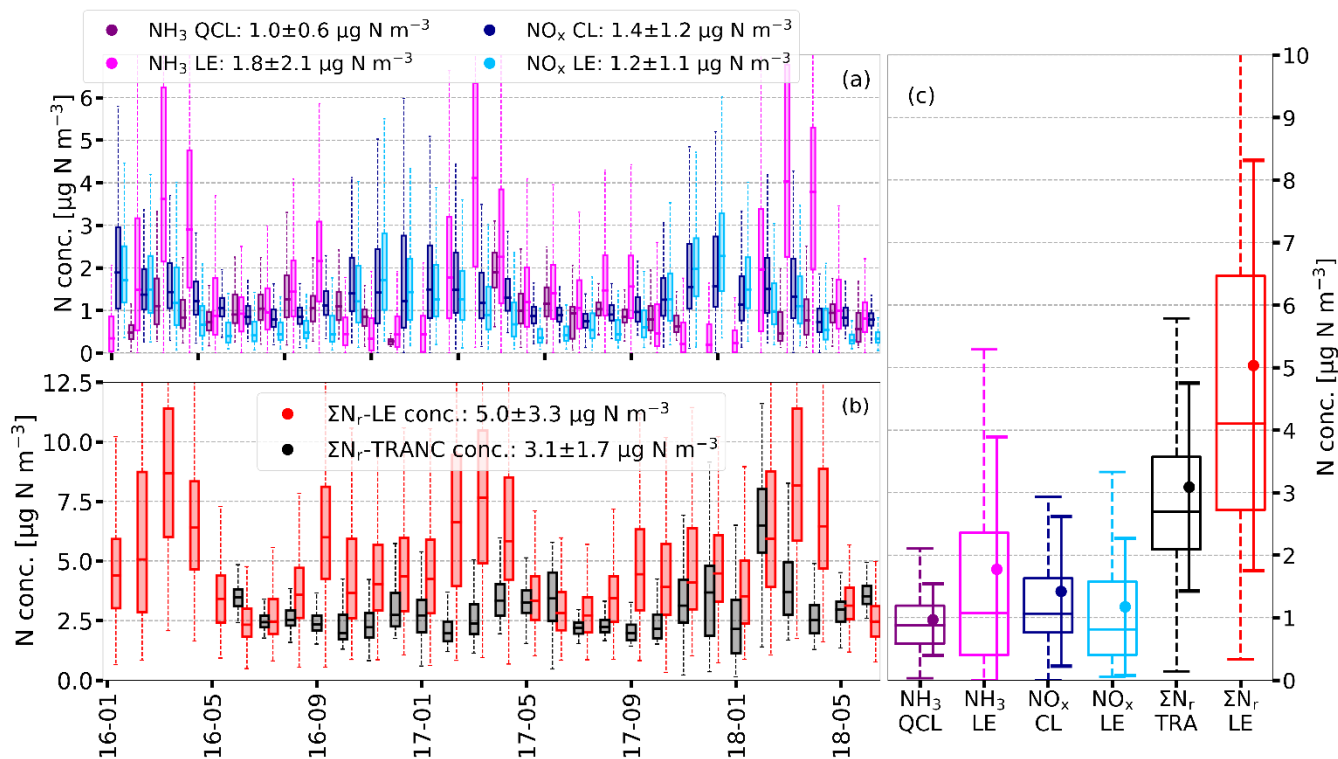
Figure 1. Half-hourly concentrations of NH₃, NOₓ, and ΣNᵣ obtained from quantum-cascade-laser (QCL), chemiluminescence (CL), and TRANC (TRA) measurements compared to LOTOS-EUROS (LE) results displayed as box-whisker plots (box frame = 25 % to 75 % interquartile range (IQR), bold line = median, whisker = 1.5*IQR) on monthly basis ((a) and (b)) and for the entire duration of the campaign (January 2016 to end of June 2018) (c) in µg N m⁻³. Darker colors represent the results from measurements, brighter colors from LOTOS-EUROS. In the legends, averages and standard deviations referring to the entire campaign for NH₃, NOₓ, and ΣNᵣ are shown.

3.1.2 Passive samplers and DELTA measurements

The large modeled NH₃ concentrations by LOTOS-EUROS could also not be verified by the observed levels of the passive samplers, and the DELTA system. Figure S1 shows a comparison of the applied NH₃ measurement techniques with NH₃ concentrations predicted by LOTOS-EUROS. A two- to threefold overestimation of NH₃ concentrations by LOTOS-EUROS is visible. In addition, the modeled seasonal pattern was also not in agreement with the results from wet chemical samplers.

A comparison of the individual measured Nᵣ compounds by DELTA to LOTOS-EUROS is displayed in Fig. 2. Considering the entire campaign, we measured average concentrations of 0.55, 0.17, 0.42, and 0.19 µg N m⁻³ for NH₃, HNO₃, pNH₄⁺, and pNO₃⁻, respectively. For the same exposure periods, the concentration averages of LOTOS-EUROS for NH₃, HNO₃, pNH₄⁺, and pNO₃⁻ were 1.8, 0.1, 1.2, and 0.8 µg N m⁻³, respectively. Differences considering the entire campaign duration are shown in Fig. S2. Like NH₃, particulate nitrogen compounds concentrations were also higher in the LOTOS-EUROS simulations. Predicted seasonality for pNH₄⁺ and pNO₃⁻ could only partially verified by DELTA measurements. For HNO₃, concentrations were in close agreement. In total, ΣNᵣ values of DELTA and TRANC showed a reasonable agreement and ΣNᵣ concentrations showed only small seasonal differences whereas LOTOS-EUROS overestimated ΣNᵣ of the TRANC by ca. 2 µg N m⁻³ (Fig. S2).
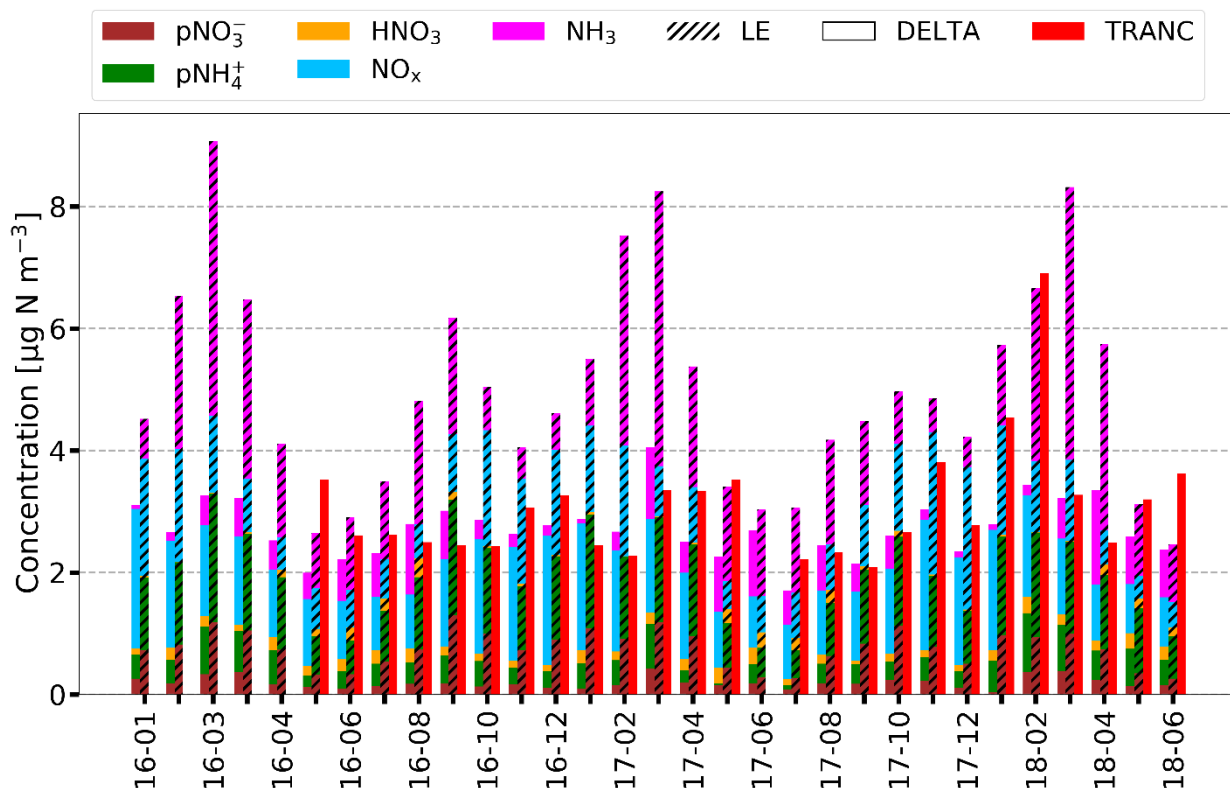
Figure 2. Monthly stacked concentration of LOTOS-EUROS (LE) (hatched), TRANC (red), DELTA, and NO_x in µg N m^{-3} for the entire measurement campaign. Gaps in the NH_3 timeseries caused by a low pump flow of the denuder pump were filled with passive sampler values from 30 m. This procedure was done for December 2016 and 2017, March 2018, and April 2018. Remaining gaps in the time series of HNO_3, pNH_4^+, and pNO_3^- were replaced by monthly averages estimated from other years if available. In case of NH_3, the procedure was applied to January 2017. For the other compounds, the gap-filling was done for December 2017, March 2018, and April 2018. Results from LOTOS-EUROS, TRANC, and NO_x measurements were averaged to the exposure periods of the DELTA samplers.

According to Wintjen et al. (2022), NO_x was the predominant compound in the ΣN_r concentrations. For the entire campaign, NO_x contributed 51.4 % and NH_3 20.0 % to measured ΣN_r, whereas LOTOS-EUROS predicted NH_3 as the most important compound (~ 35.7 %) contributing to ΣN_r followed by pNH_4^+ (~ 24.3 %), NO_x (~ 22.8 %), pNO_3^- (~ 15.2 %), and HNO_3 (~ 1.9 %) as shown by Fig. S3. Furthermore, LOTOS-EUROS showed deviations from measurements in seasonal contributions. During winter, the contribution of NH_3 to ΣN_r was surprisingly high (28.6 %) compared to the observations (4.9 %) during winter. HNO_3 contributions were comparable and on a low level between LOTOS-EUROS and DELTA. On average, particle contribution was higher in the model. Contributions of pNO_3^- and pNH_4^+ were highest during spring according to measurements but lowest in LOTOS-EUROS in that season. Apart from springtime, seasonal contributions of pNO_3^- and pNH_4^+ were higher by 6.6 to 14.4% in LOTOS-EUROS.

3.2 Comparison of modeled and measured deposition velocities

3.2.1 Comparison of modeled and measured deposition velocities for each N_r compound

NH_3 deposition velocities of LOTOS-EUROS and DEPAC-1D exhibited similar values in winter, but disagreements were found in summer and autumn. In summer, DEPAC-1D determined systematically larger median deposition velocities, whereas LOTOS-EUROS predicted a large variability in NH_3 deposition velocities during autumn, which was not supported by DEPAC-1D. For NO_2, deposition velocities of LOTOS-EUROS and DEPAC-1D agreed well in their temporal pattern and the median deposition velocities, but the variability in DEPAC-1D deposition velocities was slightly higher during summer. In both model applications, NO deposition velocities were practically zero (medians always < 0.06 cm s^{-1}). For pNH_4^+, deposition velocities of DEPAC-1D and LOTOS-EUROS agreed well with median deposition velocities close to zero, but a large disagreement was found during winter. Deposition velocities of pNO_3^- were close to zero during the entire campaign in

DEPAC-1D, but LOTOS-EUROS showed a large scattering of v_d in the winter months. For HNO$_3$, a discrepancy in v_d was also found during winter, and, similar to NH$_3$, deposition velocities of DEPAC-1D were generally larger from May to September. The comparison of the deposition velocities for each N$_r$ compound modeled by DEPAC-1D and LOTOS-EUROS is shown in Fig. S4.

3.2.2 Comparison of modeled and measured ΣN_r deposition velocities

A comparison of the modeled and measured v_d for the ΣN_r flux is provided in Fig. 3. The modeled total nitrogen dry deposition velocities were obtained by dividing the modeled dry deposition flux for all compounds by the modeled total nitrogen concentrations in ambient air. Subtracting median v_d of TRANC from LOTOS-EUROS results, differences typically ranged between -0.3 and 1.0 cm s^{-1}. Especially during the summer months, an overestimation of v_d by DEPAC-1D was observed with respect to TRANC measurements. During those months, median v_d of DEPAC-1D was ca. 2 to 3 times higher than their measured entities. LOTOS-EUROS v_d of the ΣN_r flux were generally lower than DEPAC-1D but still larger than found in the measurements within that period. During the winter months, DEPAC-1D ΣN_r showed lowest median values and variability, whereas deposition velocities of TRANC and LOTOS-EUROS were comparable caused by influence of pNO$_3^-$ and pNH$_4^+$ on LOTOS-EUROS v_d predictions.
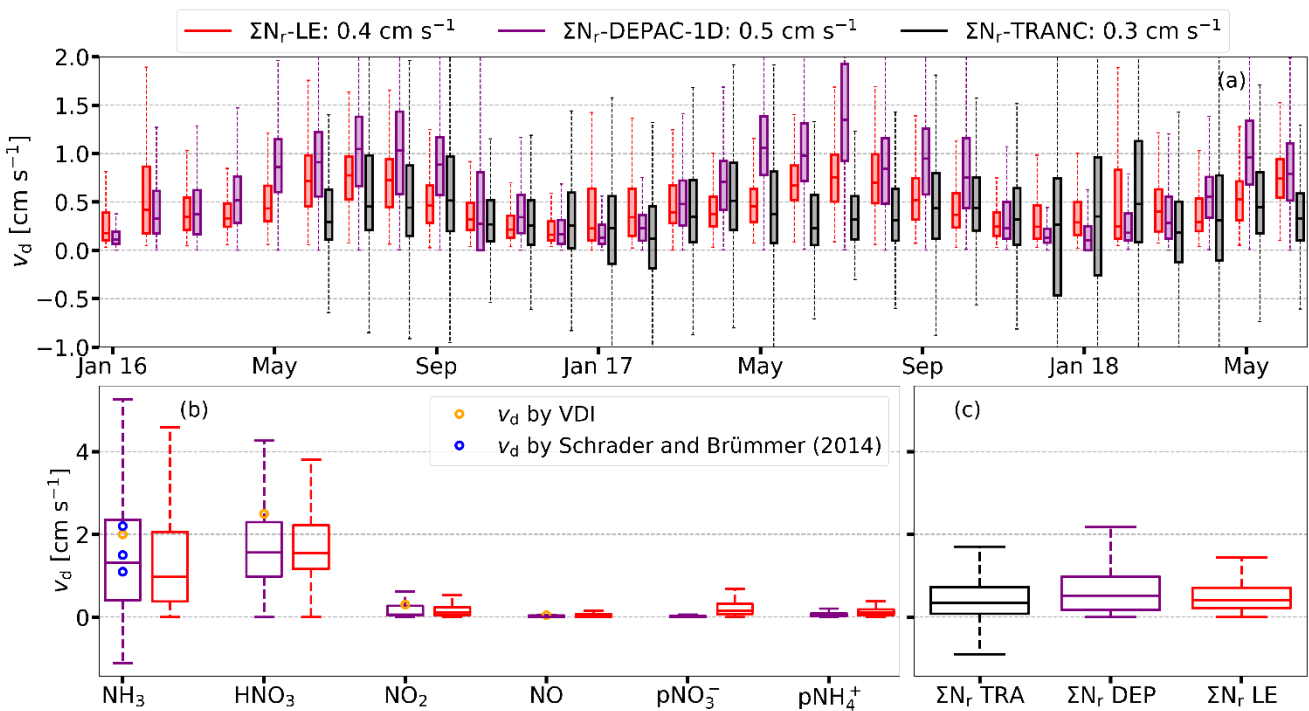
Figure 3. Monthly v_d of ΣN_r determined from TRANC (black) measurements, DEPAC-1D (purple), and LOTOS-EUROS (red) with the corrected land-use weighting in cm s^{-1} represented as box-and-whisker plots in the upper panel (a). In the corresponding legend median v_d related to the entire campaign are given. In the lower panels ((b) and (c)), box-and-whisker plots of v_d for each N$_r$ compound and ΣN_r are shown based on the entire campaign (TRA=TRANC, DEP=DEPAC-1D, LE=LOTOS-EUROS). Blue circles are referring to NH$_3$ deposition velocities reported by Schrader and Brümmer (2014) for deciduous forest, mixed forest, and spruce forest (from low to high), orange circles show deposition velocities proposed by VDI (2006).

Inspection of the diurnal cycles of ΣN_r deposition velocities for May to September in the year 2017 (Fig. S7) shows that both, the DEPAC-1D and measured data, exhibit a clear diurnal pattern with lowest deposition during the night and highest values around noon. However, in those periods where the measured data are close to zero during the night, the modeled fluxes show considerable nighttime exchange.

To further examine the reasons behind these discrepancies, we show the diurnal cycles of v_d after classifying the ΣN_r deposition velocities for half-hours without precipitation during May-September in two groups being below or above the median temperature (T_{air} =14.6°C), relative humidity (RH =74.0%), and total ΣN_r concentration (c(ΣN_r) =2.7 µg N m^{-3}). Leaf surface

wetness was measured at the site with sensors attached to a spruce and a beech tree. In order to classify the sensor as dry or wet, the half-hourly leaf wetness value was compared to a threshold value based on the calculation scheme given by Wintjen et al. (2022).

The diurnal cycles illustrate the same diurnal biases as discussed above. Figure 4 shows that DEPAC-1D results indicate that lower temperatures, higher relative humidity, and wet leaf surfaces enhance the ΣN_r dry deposition velocity. This behavior was expected based on the models' parameterization, but it is in contradiction to the TRANC measurements. Especially, the differences for the relative humidity regimes are remarkable. Smaller differences are observed for the dependency on temperature and the ΣN_r concentration, although both have a stronger influence in the model than on their measured counterpart.
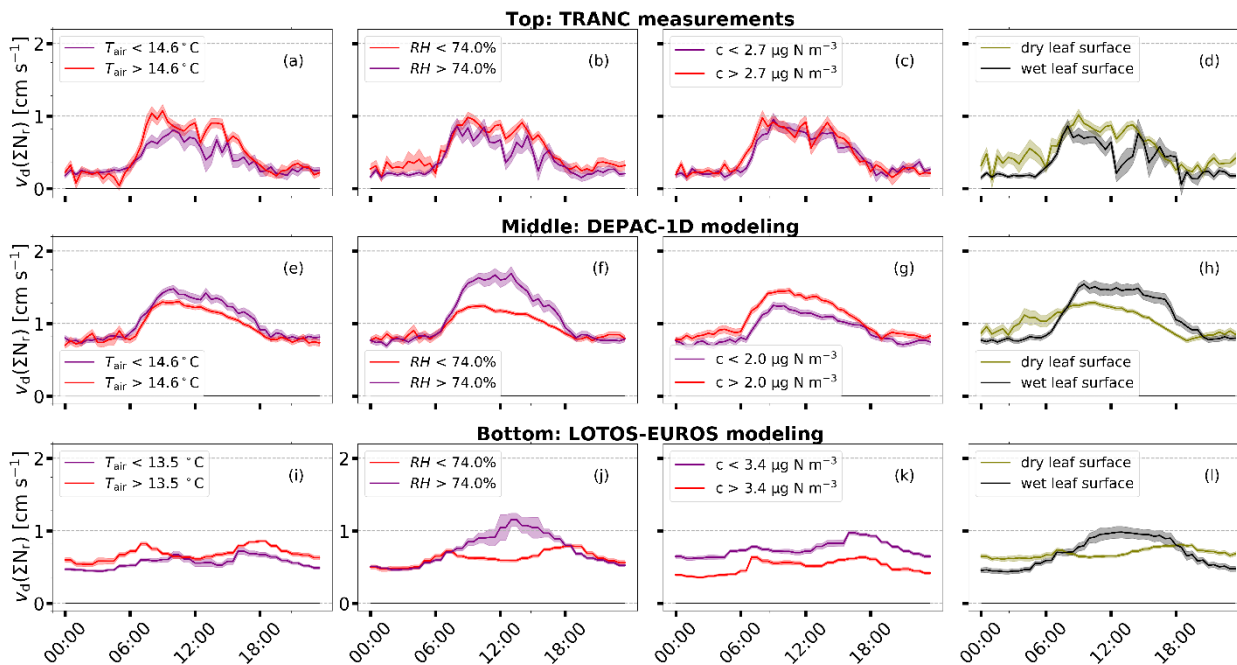
Figure 4. Averaged diurnal cycles of ΣN_r v_d for low and high temperature, relative humidity, concentration during the time frame May to September. The top row refers to TRANC measurements ((a) to (d)), the middle row refers to DEPAC-1D modeling ((e) to (h)), and the bottom row to LOTOS-EUROS simulations ((i) to (l)). Data was stratified after their median calculated for the entire period. Dry and wet leaf surfaces (Panel (d) , (h) and (l)) were identified following the calculation scheme of Wintjen et al. (2022). Shaded areas represent the standard error of the mean.

In case of LOTOS-EUROS, separating diurnal cycles of v_d led to similar observations made for DEPAC-1D regarding relative humidity and leaf surfaces. In addition, lower temperatures and concentration tend to increase v_d, which contradicts the results of DEPAC-1D. Generally, values of v_d are closer to TRANC deposition velocities, but the diurnal pattern differs from those of TRANC and DEPAC-1D showing maxima in the morning (~06:00 LT) and evening (~18:00 LT) and low values around noon except for high relative humidity and wet leaf surfaces.

3.3 Comparison of modeled and measured fluxes

3.3.1 Influence of input concentrations and meteorology on modeled fluxes

The statements made for v_d can be transferred to the flux predictions. Differences to the observations made for v_d (Fig. S4) are related to the concentration input data. For example, due to overestimations of modeled NH_3 concentrations in spring and autumn, differences in fluxes were higher during the same time. Modeled NO_2 and HNO_3 concentrations of LOTOS-EUROS were lower than their measured values resulting in flux underestimations by LOTOS-EUROS for NO_2 and HNO_3 during summer. High modeled input concentrations of particulate nitrogen led to substantial deposition fluxes in the LOTOS-EUROS simulations. Following the model predictions, NH_3 fluxes had the largest contribution to the modeled ΣN_r flux with an average

370 flux of -12.5 and -13.0 ng N m^{-2} s^{-1} in the DEPAC-1D and LOTOS-EUROS applications, respectively, considering the entire campaign. Averaged fluxes of NO_2 and HNO_3 showed – although on a low level in absolute terms – higher deposition fluxes for DEPAC-1D, namely 2.0 and 1.3 ng N m^{-2} s^{-1}, respectively, compared to 1.2 and 0.3 ng N m^{-2} s^{-1} in case of LOTOS-EUROS. Substantial flux differences were found for particulate nitrogen. DEPAC-1D averaged fluxes were close to zero (0.9 and 0.1 ng N m^{-2} s^{-1} for pNH_4^+ and pNO_3^-, respectively), whereas LOTOS-EUROS showed substantial higher aerosol deposition with

375 averaged fluxes of 3.7 and 2.2 ng N m^{-2} s^{-1} for pNH_4^+ and pNO_3^-, respectively. The comparison of fluxes for each N_r compound of LOTOS-EUROS and DEPAC-1D is shown in Figure S5.

Apart from concentrations being responsible for differences in modeled flux estimates, other parameters may have also been contributed to the deviations. To further investigate the impacts of the input data used in the LOTOS-EUROS simulations, we made a comparison of the measured and modeled input parameters used for the dry deposition modeling of NH_3 in LOTOS-

380 EUROS (Fig. S6). The agreement of temperature and global radiation in terms of their coefficient of determination R^2 was good. We found differences of approximately 1.5°C and -6.1 W m^{-2} of modeled to measured values on average. High R^2 values were determined for the entire campaign duration using half-hourly values, namely 0.97 for temperature and 0.78 for global radiation. A slight difference was found for relative humidity during the first half of 2016. However, modeled values were higher by only 2.4 % on average, and the R^2 was still 0.67. In case of u_*, we found a systematic difference, and the seasonal

385 pattern did not agree well resulting in a lower R^2 of 0.43 compared to the other micrometeorological parameters. In particular from November 2017 to February 2018, the difference between modeled and measured u_* values was considerably large.

The largest discrepancy was found for NH_3 concentration as illustrated by Fig. 2 and S1 in detail. All of the investigated input parameters play an important role in the modeling of NH_3 exchange. In order to determine the impact of these parameters on modeled NH_3 fluxes, we calculated NH_3 fluxes for the land-use class spruce forest with DEPAC-1D by replacing a specific

390 input parameter by its measured entity while all other input data were from LOTOS-EUROS. Figure 5 illustrates the results of this comparison. Since modeled and measured values of global radiation agreed well, deposition of NH_3 is only marginally reduced if measured values were used. Using measured values of temperature as input parameter led to an increase in modeled NH_3 deposition by 0.82 kg N ha^{-1}, whereas measured relative humidity led to a decrease in modeled NH_3 deposition by 0.80 kg N ha^{-1}. We found significant differences in u_*, but considering measured values in the flux calculation leads only to a

395 reduction by 1.3 kg N ha^{-1} As expected from the analysis of Fig. S6, NH_3 concentration had the largest impact on deposition. Using measured NH_3 concentration reduced the deposition substantially by 5.3 kg N ha^{-1} compared to using modeled concentrations. All reported differences refer to the entire campaign duration.
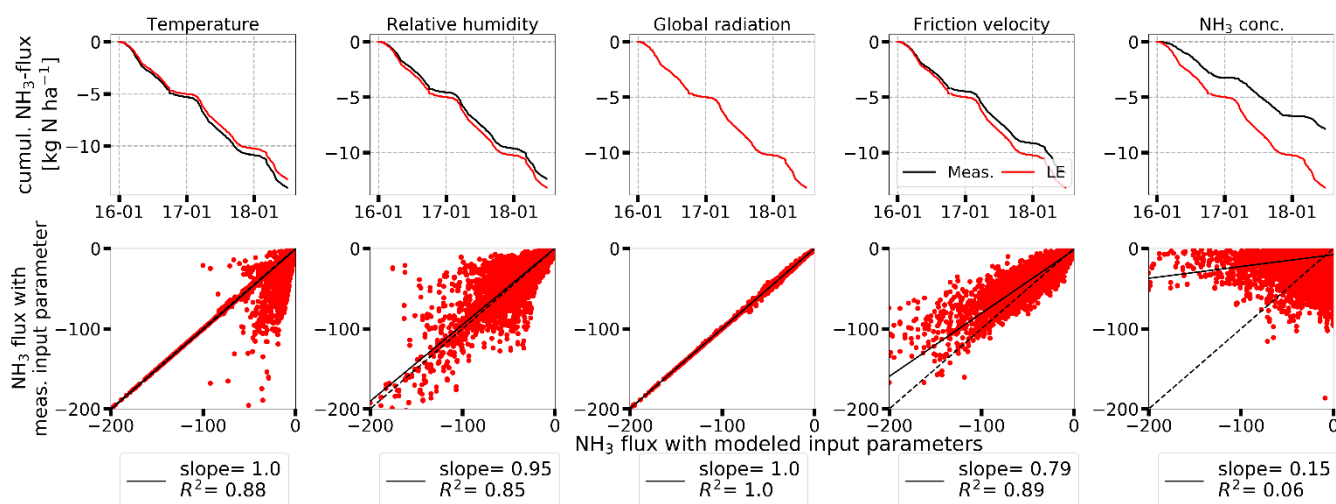
400 **Figure 5.** Comparison of NH_3 fluxes calculated with DEPAC-1D for the land-use class spruce forest based on measured (black) and modeled input data (red). The comparison was made for temperature, relative humidity, global radiation, friction velocity, and NH_3 concentrations. In the first row, NH_3 fluxes are shown as cumulative sums in kg N ha^{-1}. In the second row, scatter plots of NH_3 fluxes in ng N m^{-2} s^{-1} are given. Linear regressions are shown as black, solid lines, black, dashed lines represent 1:1 lines.

3.3.2 Comparison of modeled and measured ΣN_r deposition fluxes

The comparison of modeled ΣN_r fluxes with TRANC fluxes is presented in Fig. 6. Only periods during which high quality flux measurements were available were considered for the analysis. Models were basically able to capture the seasonal pattern of the ΣN_r fluxes well, but generally overestimated the measured flux amplitude. The ΣN_r exchange of DEPAC-1D is near zero during the entire winter, and thus the difference to measured deposition was nearly zero. During summer, a systematic overestimation of DEPAC-1D compared to measured fluxes was observed. Modeled deposition of LOTOS-EUROS was slightly lower than DEPAC-1D during summer and consequentially closer to measured fluxes. However, during autumn and spring predicted deposition of LOTOS-EUROS was significantly higher than deposition determined by DEPAC-1D and TRANC measurements due to the overestimated input NH_3 concentrations. Deposition was considerably high in LOTOS-EUROS during winter whereas median ΣN_r deposition of DEPAC-1D and TRANC was close to zero. Note that during February 2018 high aerosol concentrations were both modeled and observed. The TRANC flux data also show the impact of the aerosol deposition, but to a larger extend as LOTOS-EUROS.
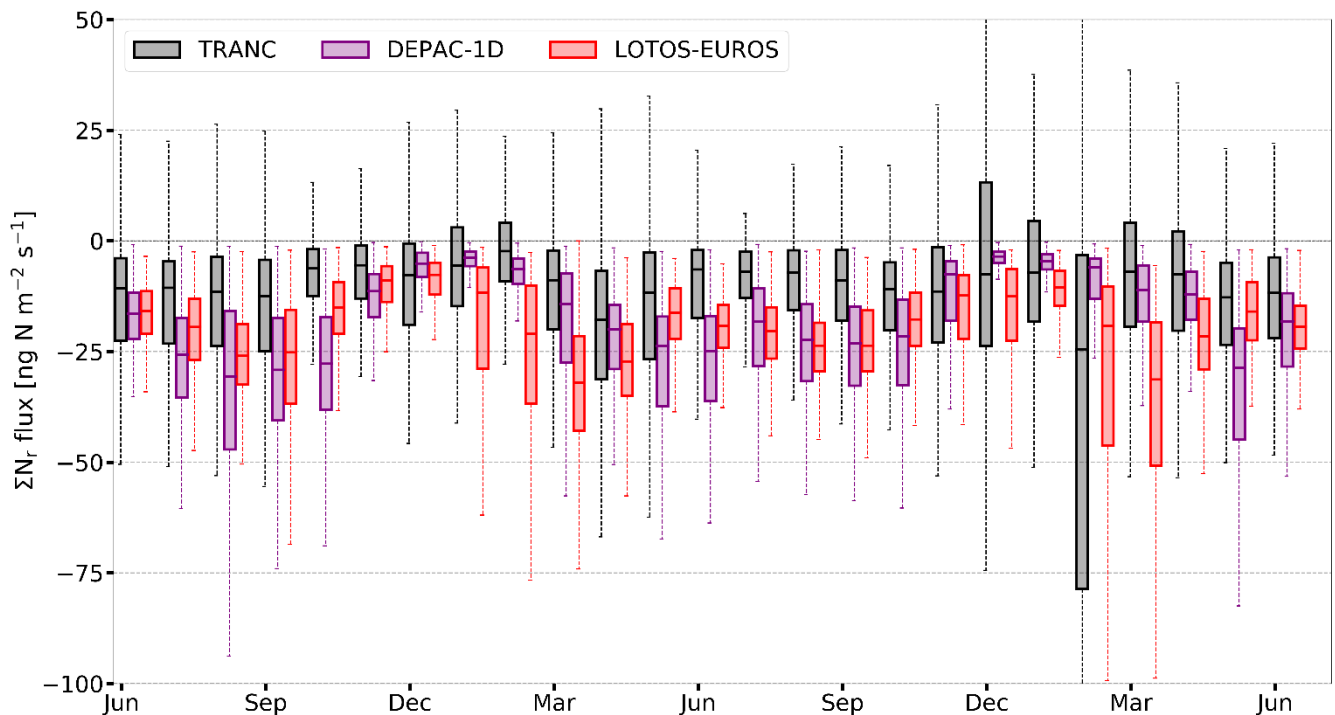
Figure 6. Fluxes of DEPAC-1D (purple), LOTOS-EUROS (red), and TRANC (black) from June 2016 to June 2018 shown as box-and-whisker plots. Whiskers of TRANC fluxes cover the range from -191 to 105 ng N m^{-2} s^{-1} in February 2018; the upper whisker of December 2017 reached 69 ng N m^{-2} s^{-1}.

Figure S8 shows exemplarily monthly diurnal cycles of ΣN_r based on TRANC, DEPAC-1D, and LOTOS-EUROS. As previously written, during winter LOTOS-EUROS overestimated deposition whereas measurements showed near-zero exchange with occasional emission phases. From May to September/October, DEPAC-1D exhibited a clear diurnal pattern with lowest deposition during the night and highest values around noon, which was in line with results from TRANC measurements. However, fluxes were systematically overestimated as indicated by Fig. 6 and Fig. S8 during those months. During the same period, ΣN_r deposition of LOTOS-EUROS was lower but still higher than TRANC fluxes except for September. During that month, LOTOS-EUROS was similar to DEPAC-1D. Generally, the diurnal deposition pattern of LOTOS-EUROS was considerably dampened, thereby not agreeing well with DEPAC-1D and TRANC..

3.4 Cumulative N exchange and method comparison

To derive annual deposition numbers the gap-filling procedures were applied to the time series of TRANC and DEPAC-1D (see Sect. 2.1). Figure 7 shows the cumulative ΣN_r dry deposition of each method from January 2016 to end of June 2018. The

contributions of the individual components to the dry ΣN_r deposition of DEPAC-1D were: 67.9 % NH_3, 15.3 % HNO_3, 10.4 % NO_2, 5.2 % NH_4^+, 1.0 % NO_3^-, and 0.1 % NO showing that modeled deposition was clearly driven by NH_3. Since emission processes could only be treated for NH_3, the observed emission of ΣN_r, for example in December 2017 (Wintjen et al., 2022), could not be sufficiently modeled. Due to issues in the parametrization of stability in LOTOS-EUROS (see Sect. 4.2.2), particle

435   deposition was enhanced in the LOTOS-EUROS results compared to DEPAC-1D (Fig. 7). Deposition of gases only was higher in DEPAC-1D due to the higher deposition velocities for NH_3, NO_2, and HNO_3 during summer compared to LOTOS-EUROS (Sect. 3.2.1). Comparing TRANC fluxes using MDV and DEPAC-1D in combination for gap-filling called TRANC(MDV+DEPAC-1D) to LOTOS-EUROS and DEPAC-1D, the differences in total dry deposition estimates were 5.4 and 2.8 kg N ha^{-1} after 2.5 years, respectively.

440
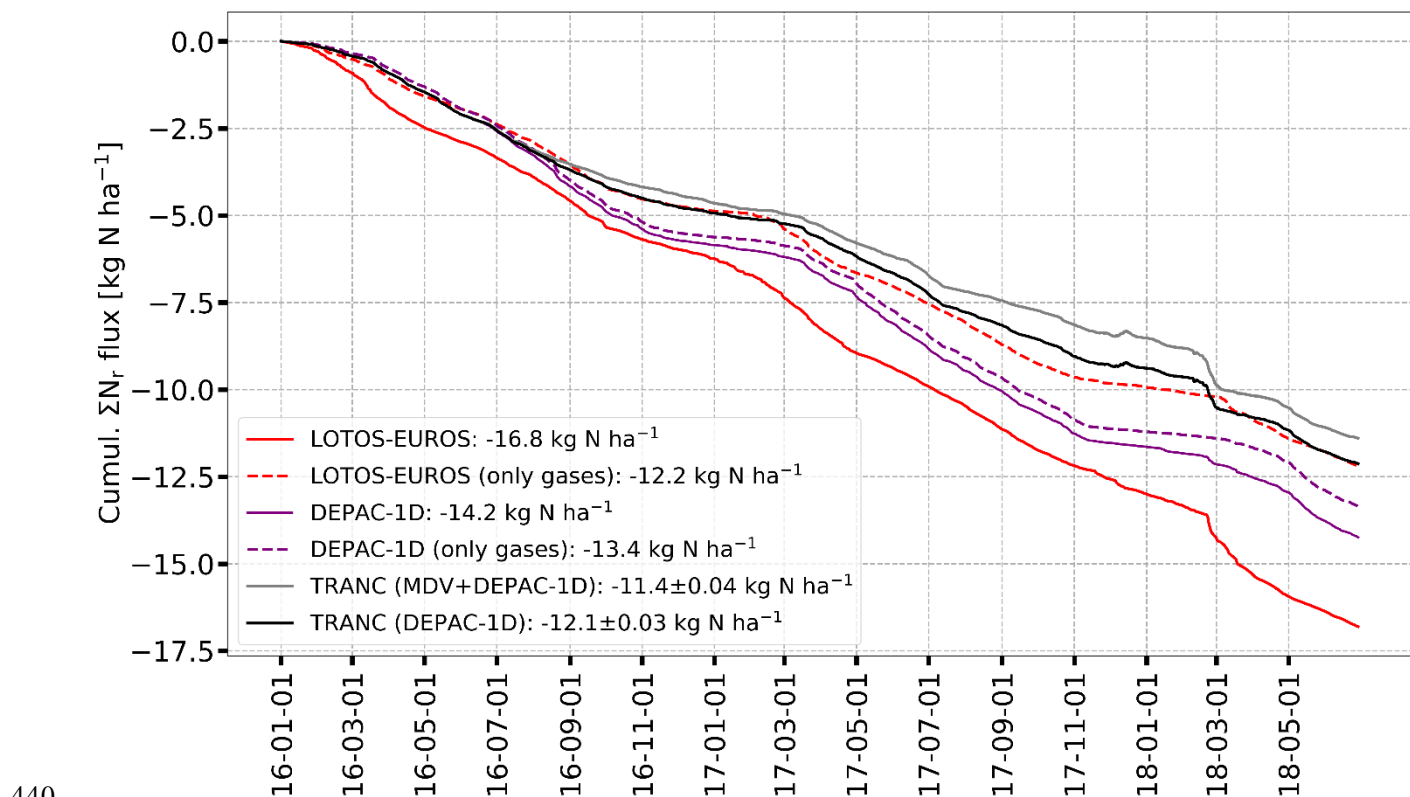
Figure 7. Comparison of measured and modeled cumulative ΣN_r dry deposition after gap-filling for the entire measurement campaign. Colors indicate different methods: TRANC+DEPAC-1D (black), TRANC+MDV+DEPAC-1D (grey), DEPAC-1D (purple), and LOTOS-EUROS (red). Dashed lines refer to cumulative dry deposition considering only gases. Number shown in the legend represent dry deposition and uncertainties after 2.5 years.

445

Since all cumulative curves exhibit generally the same shape, we conclude that the variability in fluxes is reproduced by DEPAC-1D and LOTOS-EUROS well, although the amplitude and duration of certain deposition events is different. Furthermore, both gap-filling strategies resulted in similar deposition estimates showing that the application of MDV as gap-filling tool is reasonable. Uncertainties related to gap-filling measured TRANC time series by MDV and DEPAC-1D by Eq.

450   (1) were negligible. In Fig. 8, a comparison of the ΣN_r dry deposition separated by methods and measurement years is shown. Corresponding values of the dry deposition estimates are given in Table 2.

Table 2 ΣN_r dry deposition of TRANC, DEPAC-1D, LOTOS-EUROS, and CBT for the entire measurement campaign, i.e., January 2016 to June 2018. Results from CBT were weighted according to the measured land-use weighting. For a visualization of the annual dry deposition see Fig. 8.

Method	2016 [kg N ha^{-1} a^{-1}]	2017 [kg N ha^{-1} a^{-1}]	until June 2018 [kg N ha^{-1} a^{-1}]
TRANC (MDV+DEPAC-1D)	4.6	3.9	2.9
TRANC (DEPAC-1D)	4.9	4.5	2.7
DEPAC-1D	5.8	5.8	2.6

LOTOS-EUROS	6.2	6.8	3.8
CBT (lower estimate)	3.3	4.3	
CBT (upper estimate)	6.4	7.0	

455

In 2016, annual TRANC deposition was higher than in 2017. Using only DEPAC-1D as gap-filling technique, resulted in slightly higher dry deposition estimates. In 2018, the difference to TRANC estimates until June was caused by the deposition fluxes in February 2018, which had an influence on the MDV method leading to significantly larger gap-filled fluxes. Hence, DEPAC-1D estimate was lowest among all methods for the first half of 2018. In 2016 and 2017, deposition estimates of
460 DEPAC-1D were nearly identical due to similarities in micrometeorological and concentration input values. As expected from Fig. 7, annual LOTOS-EUROS estimates were highest in comparison to DEPAC-1D and TRANC. All deposition estimates were within the range of long-term lower and upper estimates of the CBT approach estimated from 2010 to 2018, with TRANC measurements close to the lower average and LOTOS-EUROS predictions to the higher average.

465 Averaging of the annual sums of each method for 2016 and 2017 resulted in a TRANC dry deposition of 4.3±0.4 and 4.7±0.2 kg N ha^{-1} a^{-1} depending on the gap-filling approach. DEPAC-1D showed 5.8±0.1 kg N ha^{-1} a^{-1}, LOTOS-EUROS predicted 6.5±0.3 kg N ha^{-1} a^{-1}. We determined 6.7±0.3 kg N ha^{-1} a^{-1} with CBT as averaged upper estimate, and 3.8±0.5 kg N ha^{-1} a^{-1} as averaged lower estimate.

470
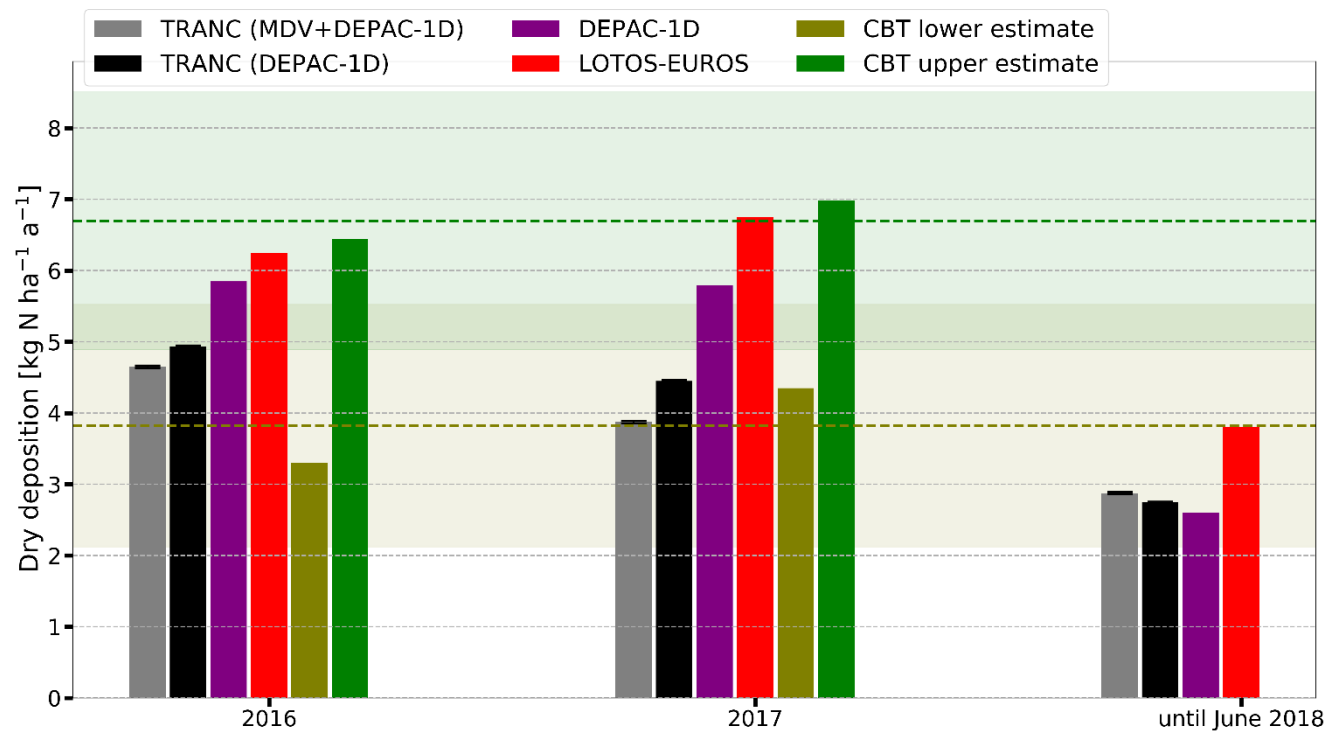
Figure 8. ΣN_r dry deposition for the years 2016 and 2017 and from January to June 2018 shown as bar chart. Colors indicate different methods: TRANC(DEPAC-1D) (black), TRANC(MDV+DEPAC-1D) (grey), DEPAC-1D (purple), LOTOS-EUROS (red), and canopy budget technique (olive and green). Data from TRANC, DEPAC-1D, and LOTOS-EUROS range from January 2016 to June 2018. CBTs' lower and upper estimates weighted according to the measured land use. The colored dashed lines indicate the averaged dry deposition of
475 the lower and upper estimates (dashed, brown line and dashed, olive line, respectively) were from 2010 to 2018, the shaded areas represent their standard deviation.

4 Discussion

4.1 Comparison of concentrations, fluxes, and annual budgets

480

Differences in the concentration contribution of N_r species to ΣN_r

According to the LOTOS-EUROS simulations, NH_3 had a predominant role in the ΣN_r concentration pattern. This result was in contrast to concentration measurements of individual N_r species at the site highlighting NO_x as the prevailing compound in the concentration pattern of ΣN_r (Wintjen et al., 2022). Moreover, the comparison of absolute concentration values revealed

485 that NH_3 was overestimated by LOTOS-EUROS explicitly during spring, and seasonal patterns of NH_3 did not agree for some periods like in autumn. NO_x concentrations agreed well in their seasonal pattern, but modeled concentrations were systematically lower.

The predominant role of NH_3 in the modeled concentrations is caused by the emission inventory used in this study. The

490 emission inventory spatially allocates NH_3 manure derived emissions through a procedure in which the animal numbers per region and agricultural land within a region are the two proxies used. Emissions from fertilizer application are allocated solely on land use. Hence, within a region all agricultural land is assumed to emit the same amount of NH_3, although the intensity of the agricultural practice and distribution of housing may vary substantially within such a region. Only south of the site, agricultural lands are located within 7 x 7 km^2 model resolution representing the site. This means that in the grid cell of the

495 model, in which the station is located, there is an emission source contributing an increased NH_3 concentration even when the wind directions are not transporting air from this agricultural region towards the station.

In LOTOS-EUROS, particulate nitrogen also had a significant contribution to modeled ΣN_r, which could not be confirmed by measurements. However, the comparison of particulate nitrogen concentrations is difficult because of the aerosol cut-off size

500 in DELTA measurements being at 4.5 μm (Tang et al., 2015). Aerosols available in fine mode like ammonium sulfate ((NH_4)$_2$$SO_4$) and ammonium nitrate ($NH_4NO_3$) are associated with aerodynamic diameter of less than 2.5 μm (Kundu et al., 2010; Putaud et al., 2010; Schwarz et al., 2016) and could be sufficiently sampled. Concentrations of coarse-mode aerosols with larger diameters than the cut-off size were partly underestimated. However, concentrations of sodium, magnesium, and calcium ions were negligible at the site (Wintjen et al., 2022) indicating that coarse-mode nitrate aerosols had no significant

505 contribution to ΣN_r concentration. In addition, carbonate coated denuders used for collecting HNO_3 overestimate concentrations by approximately 45 % since nitrous acid also sticks to those prepared surfaces (Tang et al., 2021). Thus, disagreements could be related to emission inventory of $PM_{2.5}$ and PM_{10}, chemical process modeling, or to DELTA measurements.

510 NO_x concentrations agreed in their seasonal dynamics, thus processes responsible for modeling temporal dynamics of NO_x emissions are implemented reasonably in LOTOS-EUROS. However, the systematic underestimation of NO_x concentration by LOTOS-EUROS shows that NO_x sources within this grid cell, most likely emissions from road transport and private households due to the absence of large industrial areas or power plants in the surroundings of the station, are presumably not tracked sufficiently by the emission inventory.

515

Generally, the low measured concentrations of N_r compounds show that the site was mostly outside the transport range of nitrogen enriched air masses. Improvements in the close-range transport in LOTOS-EUROS regarding atmospheric lifetime of N_r species or in the definition of atmospheric layers are likely needed. A reduction in grid cell size could lead to a more

accurate localization of potential nitrogen emission sources and a better description of close-range transport and dilution
effects. The impact of an increase in model resolution is elaborated in Sect. 4.2.2.

Differences in measured and modeled ΣN_r fluxes

Overall, measured and modeled ΣN_r deposition were comparable in the order of magnitude and partly agreed in temporal dynamics but still exhibited disagreements in flux amplitude, which were related to differences in concentration, micrometeorology, and the integration of exchange pathways in DEPAC. Currently, a compensation point is only implemented for NH_3, and thus only deposition fluxes could be modeled for other compounds. Since the total compensation point of NH_3 was negligible in DEPAC, emission fluxes of NH_3 observed for a deciduous forest by Hansen et al. (2015) probably due to a decay of fallen leaves (Hansen et al., 2013) could not be reproduced. The soil compensation point, which is integrated in the calculation of the NH_3 compensation point but currently set to zero, may reduce the observed differences to TRANC fluxes. In case of NO_2, no compensation point is implemented, and deposition on leaves is hardly allowed. Both assumptions are in disagreement with findings by Horii et al. (2004), who identified non-stomatal deposition as strongest contributor to the flux, and by Thoene et al. (1996), who proposed the existence of a compensation point for NO_2. However, nitrogen concentrations in leaf samples taken in surroundings of the site showed no unusually high enrichment of nitrogen in leaves and needles (Beudert and Breit, 2014). Thus, neglecting the emission pathway of oxidized nitrogen compounds like NO_2 seems reasonable for the measurement site.

To reduce the difference between measured and modeled fluxes, considering nitrogen emissions from soil may lead to a closer agreement with flux measurements. As written above, soil compensation point has no influence on deposition of N_r species in DEPAC yet, and soil resistance implementation is kept simple: A constant value is assumed depending on the soil wetness (dry, wet, or frozen). Improvements in the description of the exchange with the soil surface may allow to describe the observed TRANC emission fluxes in December 2017 reported by Wintjen et al. (2022). Changes made to the soil exchange path may lower the flux contribution of NH_3 as outlined before but increase the contribution NO since the latter is generally observed as emission from soil if it is produced through (de)nitrification processes (Butterbach-Bahl et al., 1997; Rosenkranz et al., 2006). At the reference height, contribution of NO may be still low due to fast conversion processes to NO_2 in the presence of ozone (O_3) within the forest canopy, especially close to the ground (Rummel et al., 2002; Geddes and Murphy, 2014). Increased NO_2 concentrations within the forest canopy may alter concentrations of various N_r species, e.g., resulting in the formation of HNO_3, which may contribute substantially to the deposition flux (Munger et al., 1996; Horii et al., 2006). Consequently, a soil compensation point may be also relevant for the exchange of other N_r species next to NH_3.

The observed large deposition fluxes in February 2018 were reproduced in the model simulations although the modeled flux amplitude was smaller. During that time, modeled concentrations and fluxes of particulate N_r were the largest contributor to total ΣN_r, leading to the assumption of particle driven ΣN_r deposition. DELTA measurements suggested that particulate NH_4^+ was most likely responsible for the measured ΣN_r deposition (Wintjen et al., 2022, Fig. 10). Modeled and measured NH_4^+ concentrations differed only by $0.75~\mu g\,N\,m^{-3}$ whereas a significant disagreement was found between NH_3 measurements and LOTOS-EUROS (approx. $2.7~\mu g\,N\,m^{-3}$). According to DELTA measurements, the NH_3 concentration was approximately 0.17 $\mu g\,N\,m^{-3}$. The averaged SO_2 concentration obtained from LOTOS-EUROS and DELTA were comparable during the exposure period of the samplers (1.5 and $2.0~\mu g\,m^{-3}$, respectively). According to the LOTOS-EUROS simulations, an excess of pNH_4^+ over pNO_3^- was modeled suggesting that particle deposition was most likely caused by pNH_4^+, which is in agreement with DELTA measurements. In conclusion, the high deposition fluxes seem to be driven by particulate NH_4^+ compounds, ammonium sulfate and ammonium nitrate. During February 2018, DELTA measurements revealed a slightly lower concentration of the SO_4^{2-} than the NO_3^- aerosol, 1.28 and $1.63~\mu g\,m^{-3}$, respectively, suggesting that NH_4NO_3 was most

responsible for the observed ΣN_r deposition fluxes. Still, the dominant aerosol is not fully known due to missing high-resolution measurements of nitrogen aerosols. Apart from February 2018, winter fluxes of LOTOS-EUROS were large compared to DEPAC-1D although the same size-resolved model for determining aerosol deposition velocities was used. By comparing dry deposition caused by gases+particles and gases only of DEPAC-1D and LOTOS-EUROS (Fig. 7), a substantial disagreement in aerosol deposition was found. The large particulate nitrogen fluxes of LOTOS-EUROS are caused by uncertainties in the stability parametrization (Sect. 4.2.2).

Analysis of ΣN_r deposition estimates

The ΣN_r dry deposition estimates of TRANC, DEPAC-1D, and LOTOS-EUROS were in the same range after 2.5 years but differences in seasonal flux patterns were found. In addition, both gap-filling methods applied to flux measurements led to similar dry deposition estimates indicating that the MDV approach is suitable for gap-filling of short-term gaps in TRANC flux timeseries. During summer, we found differences in the gap-filled fluxes due to systematic overestimation of DEPAC-1D, which was related to the different response of DEPAC-1D to micrometeorological conditions compared to TRANC (Fig. 4). It should be kept in mind that monthly integrated pNO_3^-, pNH_4^+, and HNO_3 concentration estimates may not be able to fully capture local events. Moreover, the aerosol cut-off size of DELTA was probably lower than of the TRANC measurements as supposed by Wintjen et al. (2022). Saylor et al. (2019) also noted that v_d of particles for forest are highly uncertain. Thus, differences to measurements and predictions of LOTOS-EUROS in particle deposition could be expected. Besides missing emission fluxes in DEPAC-1D, the agreement of the dry deposition estimates was reasonable indicating that an inferential model like DEPAC-1D can be a valuable alternative to purely statistical gap-filling tool at sites or seasons with predominant N deposition.

Annual dry deposition estimates from TRANC, LOTOS-EUROS, and DEPAC-1D were found to be within the range of the lower and upper estimates of the CBT approach. Adding the wet-only deposition results reported in Wintjen et al. (2022) to determined dry depositions, we calculated annual total depositions ranging between 11.5 and 14.8 kg N ha^{-1} a^{-1} noted in Table 3 for each year.

Table 3 Annual ΣN_r deposition of TRANC, DEPAC-1D, LOTOS-EUROS, and CBT for 2016, 2017, and from January to June 2018 in kg N ha^{-1} a^{-1}. Wet-only depositions of NO_3^-, NH_4^+, and DON were adapted from Wintjen et al. (2022).

Method	2016 [kg N ha^{-1} a^{-1}]	2017 [kg N ha^{-1} a^{-1}]	Until June 2018 [kg N ha^{-1} a^{-1}]
TRANC (MDV+DEPAC-1D)	12.9	11.7	6.3
TRANC (DEPAC-1D)	13.1	12.3	6.2
DEPAC-1D	14.1	13.6	6.1
LOTOS-EUROS	14.4	14.6	7.3
CBT (upper estimate)	11.5	12.2	
CBT (lower estimate)	14.6	14.8	

Comparing the results obtained from the measurement site to results obtained for other forest ecosystems using a similar validation procedure is rather difficult due to a large temporal and spatial variability in N_r compounds contributing to ΣN_r. Additionally, micrometeorological measurements as carried out in this study require substantial effort in maintenance and processing of the acquired data. Thus, most currently available EC measurements are limited to time periods covering a few weeks or months and are only available for certain locations.

Recently, Ahrends et al. (2020) compared deposition estimates of a CBT approach, an inferential method, and LOTOS-EUROS for several forest ecosystems. However, their CBT based on the variant suggested by Ulrich (1994), which is different to the version used in this study, and their inferential method (IFM) was only applied to NO_2 and NH_3 due to the limited availability

of ambient concentration measurements for other N_r compounds. In addition, deposition velocities for NO_2 and NH_3 were calculated based on literature research for different forest types accompanied by various correction factors. They reported similar annual dry deposition estimates for CBT and IFM, which were found to be 12.6 and 12.9 kg N ha^{-1} a^{-1}, respectively. Minimum dry deposition was 3.8 kg N ha^{-1} a^{-1} for CBT and 1.0 kg N ha^{-1} a^{-1} for IFM. The lowest average dry deposition was 9.3 kg N ha^{-1} a^{-1} given by LOTOS-EUROS but its minimum dry deposition was highest (approx. 6.3 kg N ha^{-1} a^{-1}). Since we measured N deposition in a low-polluted environment, the agreement to the minimum dry deposition estimates of Ahrends et al. (2020) seems reasonable.

In the consideration of critical loads, total nitrogen deposition is within the proposed limits. Critical loads ranging from 10 to 15 kg N ha^{-1} a^{-1} and 10 to 20 kg N ha^{-1} a^{-1} were defined by Bobbink and Hettelingh (2011) for *Picea abies* and *Fagus sylvatica*, respectively. Since *Picea abies* was the prevailing tree species in the flux footprint (approx. 80%), the critical load of the investigated forest ecosystem is probably closer to the limits of *Picea abies*. The state of tree physiological parameters suggested that the critical load concept, which indicated that the exposure of the forest to N deposition is still below critical limits, is a valuable tool to evaluate the functionality of an ecosystem. Long-term observations of nitrogen input to this ecosystem showed nitrogen concentrations in trees and water reservoirs, but ecosystem functionality was not impaired. According to leaf examinations done by Beudert and Breit (2014) at the site, balanced ratios of nitrogen to other nutrient concentrations in tree foliage were found, and usual tree growths were reported. Jung et al. (2021) found low nitrate concentrations in soil water, aquifers, and streams at the site showing an intact nitrogen retention and storage system. Moreover, green algae coatings on spruce needles usually indicating higher NH_x dry deposition (Grandin, 2011) were not found at the site.

4.2 Modeling uncertainties

Influence of micrometeorological parameters

In both DEPAC-1D and LOTOS-EUROS, wet leaf surfaces and high relative humidity were identified as conditions enhancing ΣN_r deposition from May to September. In case of temperature, dry leaf surfaces, and low relative humidity, diurnal cycles of v_d showed a different behavior: For DEPAC-1D, lower temperatures were found to increase v_d, whereas the opposite observation was made for LOTOS-EUROS and their shapes were different. Deposition velocities of DEPAC-1D reached highest values around noon and decreased towards evening. LOTOS-EUROS predicted highest values in the morning and evening, but deposition velocities exhibited a decreasing trend towards noon. These disagreements were probably related to the stomatal uptake of NH_3 prevailing in the ΣN_r deposition flux of LOTOS-EUROS. Only for wet leaf surfaces and high relative humidity, which generally hold an important role in the deposition of NH_3 (Wentworth et al., 2016), diurnal shapes of DEPAC-1D and LOTOS-EUROS were similar suggesting that cuticular deposition of NH_3 seemed to be most responsible for the modeled ΣN_r dry deposition at the measurement site. Similar observations were made by Wyers and Erisman (1998), who identified the cuticular pathway as a larger sink for NH_3 than the stomatal pathway.

However, the results from TRANC measurements highlighted higher temperatures, lower relative humidity, and dry leaf surfaces as important factors enhancing ΣN_r deposition, and diurnal cycles of the TRANC were different in shape from those of LOTOS-EUROS. In addition, night-time deposition velocities of the TRANC were close to zero, whereas modeled deposition velocities were between 0.5 and 1 cm s^{-1}. The differences are probably related to low aerodynamic resistances in the model applications indicating high u_* values, which could not be verified by EC measurements. However, measuring night-time exchange with the EC method and micrometeorological methods in general is challenging. Common detection algorithms for a u_* threshold (Reichstein et al., 2005; Barr et al., 2013) are not applicable to N_r species yet since they are optimized for CO_2. The contradiction in wet and dry conditions lead to the assumption that the current implementation of the NH_3 exchange

640 pathways in DEPAC was not fully suited for predicting NH_3 deposition correctly and needs further investigation. It should be kept in mind that we measured ΣN_r exchange at a low-polluted, mixed forest site. Sites with different micrometeorology, vegetation, and pollution climate may exhibit other parameters like surface wetness, canopy temperature, and ambient concentration responsible for the ΣN_r exchange as found by Milford et al. (2001). Further comparisons to flux measurements of ΣN_r and NH_3 are needed to investigate the role of stomatal and cuticular deposition.

645

Influence of soil resistance and soil compensation point

In DEPAC, soil resistance is set to a constant value depending on soil status, i.e. frozen ($R_{soil}=1000\,s\,m^{-1}$), dry ($R_{soil}=100\,s\,m^{-1}$), or wet ($R_{soil}=10\,s\,m^{-1}$). In addition, the in-canopy resistance (as part of the effective soil resistance) is dependent on the inverse of u_*, surface area index (LAI+ area index of stems and branches (van Zanten et al., 2010)) and may lower the exchange

650 with the soil. A soil compensation point is currently set to zero for NH_3 and not implemented for other N_r species since an appropriate parametrization or value is not known so far as argued by van Zanten et al. (2010). Consequently, deposition through the soil pathway is close to zero for most half-hourly records according to the current parametrization. Including a soil compensation point in DEPAC and improvements in the soil resistance parametrization, may lead to a better agreement with flux measurements. However, modifications related to soil exchange are probably challenging since they may affect the

655 contribution of various N_r species to the ΣN_r flux, and a parametrization of soil resistance, e.g., depending on soil moisture and temperature, is probably required instead of assuming a constant value.

At the site, no measurements of soil conductance, soil moisture, and soil temperature were made. Thus, we cannot evaluate the representativeness of the current soil parametrization. Moreover, those measurements would have been challenging at the

660 site due to the large spatial variability in the wide flux foot print area. For further measurement campaigns of similar nature, measurements of soil specific parameters are highly recommended.

Cuticular compensation point of NH_3

Schrader et al. (2016) discovered problems in the calculation of the cuticular NH_3 compensation point under high ambient NH_3

665 concentrations and high temperatures, for instance during summer. The current implementation of Wichink Kruit et al. (2010) in DEPAC likely underestimates the cuticular compensation point at high temperatures. This issue is not solved yet and could not be verified for our measurement site due to generally low NH_3 concentrations and the implementation of monthly averaged NH_3 concentration instead of half-hourly values in the concentration time series of NH_3 to some extent. Moreover, the cuticular emission potential was estimated from monthly averaged concentrations in LOTOS-EUROS and DEPAC-1D, instead of

670 instantaneous values as in the original parameterization of Wichink Kruit et al. (2010), likely somewhat alleviating the issue discussed in Schrader et al. (2016). Thus, this issue could not be the main reason for the difference to flux measurements at our site.

Influence of emission fluxes on ΣN_r

675 With the TRANC system, the contribution of ΣN_r emission fluxes above the limit of detection was estimated to 16 % (Wintjen et al., 2022). Unfortunately, robust QCL-based NH_3 flux measurements using the EC method were not possible at the measurement site (Wintjen et al., 2022). Thus, contribution of individual N_r species – at least the NH_3 and hence the reduced N contribution - to the measured ΣN_r flux is not known. However, the presence of emission fluxes shows that an implementation of a compensation point for soil and/or mechanisms describing emissions of oxidized N_r species like NO_2 and

680 HNO_3 should be considered. As described above, fully integrating the soil compensation point in the exchange of NH_3 may explain emissions fluxes of ΣN_r. For HNO_3, emission fluxes were reported in recent publications (Tarnay et al., 2002; Farmer and Cohen, 2006, 2008). The latter conducted flux measurements of HNO_3 above a pine forest and found a significant

contribution of emission fluxes during summer. Those emission could also be induced by the evaporation of NH_4NO_3 from leaf surfaces occurring at higher temperatures (Wyers and Duyzer, 1997; Van Oss et al., 1998), or particles deposited or formed on leaf surfaces as discussed by Nemitz et al. (2004). Emission fluxes of NO and NO_2 were reported in several publications, e.g., Farmer and Cohen (2006), Horii et al. (2004), and Min et al. (2014) leading to the assumption of the existence of a compensation point (Thoene et al., 1996), whereas other authors still critically discuss such a compensation point for NO and NO_2 (Chaparro-Suarez et al., 2011; Breuninger, et al. 2013; Delaria, et al., 2018, 2020). Since no significant N concentrations in leaves were found at the site (Beudert and Breit, 2014), an integration of a compensation point for NO_2 is probably less useful for the measurement site. Still, further flux comparisons of oxidized nitrogen compounds to their modeled entities are needed which would possibly lead to improvements in the representation and accurate apportionment of exchange pathways in (bi)directional resistance models.

4.2.1 Uncertainties in DEPAC-1D

Leaf area index and displacement height

Besides the current implementation of the exchange pathways in DEPAC, deposition estimates could be more accurate if concentration measurements at a higher time resolution and measurements of the LAI would have been available. We did not take measurements of the LAI or other vegetation properties at the measurement site. Still, the interpretation of differences to flux measurements would be challenging since the vegetation inside the flux footprint was not uniform. Inside the footprint, we identified dead wood in southern direction and a mix of rather young and matured trees in easterly direction. Differences in tree age were related to a dieback by bark beetle in the mid-1990s and 2000s (Beudert and Breit, 2014) from which the forest stand is still recovering. Shifting z_0 or d by ±50 %, caused a change of +5.0 %/-3.2 % and +5.6 %/-9.1 %, respectively, in the nitrogen dry deposition after 2.5 years. An incorrect assessment of the modeled LAI by ±50 % had a significant influence on the dry deposition. It led to a change of +18.9 %/-27.2 %. It shows that in further field applications of DEPAC-1D measurements the LAI should be considered, but an incorrect assessment of the LAI would not solely explain the overestimation of DEPAC-1D to TRANC measurements.

Using long-term concentration averages

The main uncertainty of DEPAC-1D fluxes was most likely the usage of monthly integrated DELTA concentrations for the N_r compounds. Thus, the large variability in the timeseries of these compounds happened on timescales of a few seconds were not accounted in deposition modeling. Even with high-resolution measurements of the QCL, the short-term variability in NH_3 concentrations was not detectable (Wintjen et al., 2022). As stated in Sect. 2.2.3, we did not superimpose monthly concentrations values with synthetic diurnal patterns. Concentrations of N_r compounds are highly variable during the day and depend on various parameters such as turbulence, temperature, relative humidity, precipitation, and emission sources. Reproducing influences of those parameters with averaged diurnal cycles about at least weeks or months, is not possible. We found that NH_3 concentration was generally low during winter and assigned with a low variability as found by measurements. During those times, using monthly integrated averages is reasonable (Schrader et al., 2018). However, we probably overestimated modeled fluxes due to the use of monthly averaged concentrations. In order to get at least an impression which N_r compounds' fluxes are probably biased by this approach, we compared monthly averaged fluxes of LOTOS-EUROS (A1) with fluxes calculated by multiplying monthly averaged v_d with their monthly concentration averages (A2) and subsequently corrected them by applying Eq. (9) and (10) of Schrader et al. (2018). Generally, we found that all N_r compounds' fluxes were overestimated by A2 whereas the difference to A1 depends on the investigated N_r compound and season. All N_r compounds had in common that the difference between both approaches was negligible during seasons with small deposition fluxes, for example in winter. Within seasons of large deposition fluxes, significant discrepancies were found, in particular for NH_3.

Overall, mean absolute deviations to A1 were 35.0, 0.27, 0.18, 0.92, 2.5, and 2.4 ng N m^{-2} s^{-1} for NH$_3$, NO$_2$, NO, HNO$_3$, NH$_4^+$, and NO$_3^-$, respectively.

It should be considered that we used LOTOS-EUROS data for this comparison. Especially for NH$_3$, NH$_4^+$, and NO$_3^-$, their modeled seasonality and concentrations exhibited significant disagreements to DELTA measurements. Thus, the flux overestimations should be seen as highest guess. Measured high resolution concentrations would have led to lower values. Still, the comparison highlights the necessity for high-resolution measurements of N$_r$ compounds. Those measurements should be made for N$_r$ compounds, which probably prevail the exchange dynamics of ΣN$_r$ at a certain site and thereby at least cover time periods with large temporal variations in their concentrations. This procedure was performed for NH$_3$ and NO$_2$ at the measurement site and should be considered for further measurement campaigns.

4.2.2 Uncertainties in LOTOS-EUROS

The larger nitrogen deposition values for the measurement site as modeled by LOTOS-EUROS are mostly related to the overestimation of modeled input NH$_3$ concentrations. As visualized by Fig. S1, LOTOS-EUROS clearly exceed observed NH$_3$ concentrations in spring and autumn. Such an overestimation of NH$_3$ and NH$_4^+$ in precipitation at forest monitoring sites was identified before for stations in Baden-Württemberg and Bavaria (Schaap et al., 2017). A similar systematic overestimation by the model in southern Germany has also been identified in comparison to novel NH$_3$ satellite data (Ge et al., 2020). This leads us to believe that the overestimation is for a large part due to shortcomings in the emission information (Sect. 4.1), potentially in combination with the model resolution.

A reduction in grid cell size could lead to a more precise localization of potential nitrogen emission sources and a better description of close-range transport and dilution effects. For a simulation covering 2015, we were able to calculate concentrations and fluxes at a higher grid cell resolution (2 x 2 km^2) and compared the results to the standard spatial resolution (7 x 7 km^2). In case of the high grid cell resolution, concentrations were lower but only by 2 to 10 % depending on the compound compared to standard spatial resolution. For the higher grid cell resolution, annual N budget was higher than the budget of the standard spatial resolution case study, but only by 4.3 % probably due to differences in the relative fractions of land-use classes. The contribution of forest land-use classes was likely higher in case of the high spatial resolution. The higher grid cell resolution probably led to improvements in modeling atmospheric turbulence resulting in higher deposition velocities. This example shows that the grid cell resolution of 7 x 7 km^2 is not mainly responsible for the overestimation of concentrations and fluxes by LOTOS-EUROS.

Nevertheless, the seasonal cycle also indicates that the information, which LOTOS-EUROS extracts from the emission inventory, does not agree well with agricultural management practiced in the surrounding of the Bavarian Forest. The agricultural fields close to the Bavarian Forest are predominantly extensively managed grass lands. Manure application to grass lands is known to occur much more evenly distributed across the year in comparison to the application for crop production, which mainly occurs before or during the growing season. Hence, in reality the emission variability maybe prone more to summer conditions. Currently, the detailing of crop dependent emissions made within LOTOS-EUROS, i.e. the use of variable emission fractions within German regions in combination with the recent timing module of Ge et al. (2020), is under investigation to elucidate if these factors are contributing to the measurement-model mismatches observed for the measurement site.

Additional features may also contribute to the observed differences. Within LOTOS-EUROS, modeled concentrations were written out for a reference height of 2.5 m above z_0, which was lower than the measurement height of the flux tower. Slight differences between measured and modeled micrometeorological input data were found, for example the difference in relative

humidity in the first half of 2016. Differences for that time period were related to the usage of local meteorological data taken at 50 m, which was higher than the model layer height associated with air temperature and relative humidity. The deviations in u_* as illustrated in Fig. S6 and Fig. 5 were related to differences in measurement heights at which wind speeds and roughness lengths were calculated. The model grid cell consists of various vegetation types each with a unique surface roughness length. We showed that the weighting of the land use classes within the grid cell was not in agreement with the vegetation of the flux foot print affecting micrometeorological variables, e.g. u_*, L, and thereby the calculation of R_a and R_b.

The large contribution of aerosols to the total deposition (Fig. 7) modeled by LOTOS-EUROS was accompanied by unusually high deposition velocities of pNH_4^+, pNO_3^-, and HNO_3 from November 2017 to February 2018. Deposition of HNO_3 and particulate nitrogen is mostly driven by the aerodynamic resistance and quasi-laminar resistance, R_a and R_b. Since v_d of those compounds was relatively high compared to measurements during that time, R_a and R_b were probably low or even close to zero. R_a and R_b depend on various parameters like u_*, the integrated stability corrections functions after Webb (1970) and Paulson (1970), surface roughness, and leaf area index. L determines the integrated stability functions and depends on wind speed close to the surface, cloud cover, and solar zenith angle (Manders-Groot et al., 2016). Snow cover is not considered in the parametrization of L yet. Including snow cover in the parametrization affect the albedo of the surface and thus the prevailing stratification of the boundary layer, which probably leads to more occurrences of stable stratification. An implementation of snow cover in the parametrization of L may reduce the deviations of simulated vs. measured stability and u_*.

An incorrect setting of the LAI and z_0 can have a significant influence on modeled ΣN_r deposition as shown in Sect. 4.2.1. The relative changes in modeled ΣN_r deposition caused by LAI and z_0 were comparable to values presented recently by van der Graaf et al. (2020), who used satellite-derived LAI and z_0 data from Moderate Resolution Imaging Spectroradiometer (MODIS) to calculate ΣN_r deposition with LOTOS-EUROS for a grid cell size of 7×7 km^2. Overall, they observed changes in ΣN_r dry deposition ranging from -20% to +30%. However, there was almost no change in ΣN_r dry deposition and in NH_3 concentration observable for the Bavarian Forest measurement site if LAI and z_0 from MODIS were used. The attempts of van der Graaf et al. (2020) and Ge et al. (2020) did not provide a solution for the general overestimation of the NH_3 deposition above southern Germany. We assume that the spatially and temporally imprecise allocation of emission data is most responsible for the disagreement to flux measurements. Further investigations on these issues are needed.

5. Conclusions

The annual total reactive nitrogen (ΣN_r) dry deposition estimates of all methods were in the same range considering uncertainties of measured fluxes and model applications. Annual estimates from the Total Reactive Atmospheric Nitrogen Converter (TRANC) were lower than the results from an in-situ inferential modeling approach using the bidirectional resistance scheme DEPAC (Deposition of Acidifying Compounds) (here called DEPAC-1D) and the chemical transport model LOTOS-EUROS (Long Term Ozone Simulation – EURopean Operational Smog) v2.0. Annual dry deposition estimates of TRANC, DEPAC-1D, and LOTOS-EUROS were within the minimum and maximum dry deposition estimates of the canopy budget technique (CBT) showing ecological and micrometeorological measurements provide reasonable estimates. According to the critical load concept, annual nitrogen deposition was below critical values. Findings were supported by local vegetation samplings showing no indications for nitrogen exceedances leading to the conclusion that the critical load concept is a useful tool to describe the health status of an ecosystem.

Differences between DEPAC-1D and TRANC measurements could be related to uncertainties in parametrizing the exchange pathways of reactive gases, the usage of low-resolution input data, or the missing exchange pathway with soil. Modeled ΣN_r deposition velocities of DEPAC-1D were enhanced with regard to wet conditions, which was in contrast to TRANC measurements leading to systematically larger deposition fluxes. To a smaller extent, the same observation was made for

LOTOS-EUROS, and additionally deposition velocities of DEPAC-1D and LOTOS-EUROS did not agree well in their diurnal pattern. Thus, a further investigation of stomatal vs. non-stomatal deposition pathways needs to be conducted as these are likely the main factors for discrepancies in modeled vs. measured results. Besides possible uncertainty sources in DEPAC-1D,

810   measured dry deposition estimates using DEPAC-1D for gap-filling were similar showing that DEPAC-1D (and by extension, inferential modeling in general) is a valuable gap-filling tool at sites with prevailing N deposition. The difference to dry deposition estimates of LOTOS-EUROS was mainly related to an overestimation of NH_3 concentrations by a factor of two to three compared to measured concentrations. Consequently, NH_3 contributed most to the ΣN_r concentration pattern in LOTOS-EUROS whereas NO_x was identified as predominant compound by measurements. The imprecise allocation of emission data

815   may be responsible for the discrepancies to measured NH_3 concentrations since the general overestimation of NH_3 concentrations by LOTOS-EUROS has still not been solved by attempts of model developers (van der Graaf et al., 2020; Ge et al., 2020).

Further comparisons of flux measurements and model applications are needed to investigate exchange characteristics of ΣN_r and its individual compounds, if possible, simultaneously and at different ecosystems. Measuring several N_r compounds and

820   ΣN_r at a high time resolution is probably not affordable due to operating and maintenance costs, high technical requirements, and time-consuming processing of the acquired data. A solution could be continuous monitoring of N_r compounds by low-cost samplers complemented by high-frequency measurements of ΣN_r and selected compounds like NH_3 for a limited time, which will result in a better understanding of exchange processes and thus in an improvement of deposition models (cf. Schrader et al., 2020).

825

Code and data availability. All data are available upon request from the first author of this study (pascal.wintjen@thuenen.de). Concentration, flux, and micrometeorological data from measurements and ecological information about the site are included

830   in the following repository: https://zenodo.org/record/5841074 (Brümmer et al., 2022a). Also, Python 3.7 code for flux data analysis can be requested from the first author.

835   *Author contributions.* PW, FS, MS, and CB conceived the study. PW wrote the manuscript, carried out the measurements at the forest site, and the comparison of measured and modeled flux data and interpretation. FS evaluated meteorological measurements and set up DEPAC-1D. MS and RK provided insights in interpreting LOTOS-EUROS results. BB conducted canopy throughfall and wet deposition measurements. CB installed the instruments at the site. The results were thoroughly discussed with all authors, and FS, MS, BB, RK, and CB contributed to the manuscript.

840

Competing interests. The authors declare that they have no conflict of interest.

845

Acknowledgements. We thank Undine Zöll for scientific and logistical help to the measurements, Jeremy Rüffer and Jean-Pierre Delorme for excellent technical support, Ute Tambor, Andrea Niemeyer, and Dr. Daniel Ziehe for conducting laboratory

analyses of denuder and filter samples, and the Bavarian Forest Nationalpark (NPBW) Administration, namely Wilhelm Breit
and Ludwig Höcker for technical and logistical support at the measurement site.

Financial support. This work has been funded by the German Environment Agency (UBA) (project FORESTFLUX, support code FKZ 3715512110) and by the German Federal Ministry of Education and Research (BMBF) within the framework of the Junior Research Group NITROSPHERE (support code FKZ 01LN1308A).

References

Ahrends, B., Schmitz, A., Prescher, A.-K., Wehberg, J., Geupel, M., Henning, A., and Meesenburg, H.: Comparison of Methods for the Estimation of Total Inorganic Nitrogen Deposition to Forests in Germany, Frontiers in Forests and Global Change, 3, 1-22, doi:10.3389/ffgc.2020.00103, 2020.

Ammann, C., Wolff, V., Marx, O., Brümmer, C., and Neftel, A.: Measuring the biosphere-atmosphere exchange of total reactive nitrogen by eddy covariance, Biogeosciences, 9, 4247–4261, doi:10.5194/bg-9-4247-2012, 2012.

Ammann, C., Jocher M., and Voglmeier, K.: Eddy Covariance Flux Measurements of NH_3 and NO_y with a Dual-Channel Thermal Converter," *IEEE International Workshop on Metrology for Agriculture and Forestry (MetroAgriFor)*, pp. 46-51, doi: 10.1109/MetroAgriFor.2019.8909278, 2019.

Barr, A., Richardson, A., Hollinger, D., Papale, D., Arain, M., Black, T., Bohrer, G., Dragoni, D., Fischer, M., Gu, L., Law, B., Margolis, H., McCaughey, J., Munger, J., Oechel, W., and Schaeffer, K.: Use of change-point detection for friction–velocity threshold evaluation in eddy covariance studies, Agricultural and Forest Meteorology, 171–172, 31–45, doi: 10.1016/j.agrformet.2012.11.023, 2013.

Beudert, B. and Breit, W.: Kronenraumbilanzen zur Abschätzung der Stickstoffgesamtdeposition in Waldökosysteme des Nationalparks Bayerischer Wald, techreport, Umweltbundesamt, Dessau-Roßlau, Germany, available at: https://www.umweltbundesamt.de/sites/default/files/medien/370/dokumente/kronenraumbilanzen_stickstoffgesamtdepositio n_nationalpark_bayerisches_wald_-_berichtsjahr_2013_im_forellenbach.pdf (last access: 14 March 2022), 2014.

Bobbink, R., Hornung, M. and Roelofs, J. G. M.: The effects of air-borne nitrogen pollutants on species diversity in natural and semi-natural European vegetation, Journal of Ecology, 86, 717–738, doi:10.1046/j.1365-2745.1998.8650717.x, 1998.

Bobbink, R. and Hettelingh, J.-P.: Review and revision of empirical critical loads and dose-response relationships. National Institute for Public Health and the Environment (RIVM), RIVM Report, https://www.rivm.nl/bibliotheek/rapporten/680359002.pdf (last access: 14 March 2022), 2011.

Breuninger, C., Meixner, F. X., and Kesselmeier, J.: Field investigations of nitrogen dioxide (NO_2) exchange between plants and the atmosphere, Atmospheric Chemistry and Physics, 13, 773–790, doi:10.5194/acp-13-773-2013, 2013.

Brümmer, C., Marx, O., Kutsch, W., Ammann, C., Wolff, V., Flechard, C. R., and Freibauer, A.: Fluxes of total reactive atmospheric nitrogen (ΣN_r) using eddy covariance above arable land, Tellus B: Chemical and Physical Meteorology, 65, 19770, doi:10.3402/tellusb.v65i0.19770, 2013.

Brümmer, C., Rüffer, J. J., Delorme, J.-P., Wintjen, P., Schrader, F., Beudert, B., Schaap, M., and Ammann, C.: Reactive nitrogen fluxes over peatland and forest ecosystems using micrometeorological measurement techniques, Earth System Science Data, 14, 743-761, doi:10.5194/essd-14-743-2022, 2022.

Brümmer, C., Rüffer, J. J., Delorme, J.-P., Wintjen, P., Schrader, F., Beudert, B., Schaap, M., and Ammann, C.: Reactive nitrogen fluxes over peatland (Bourtanger Moor) and forest (Bavarian Forest National Park) using micrometeorological measurement techniques (1.1) [Data set]. Zenodo. doi:10.5281/zenodo.5841074, 2022a.

Butterbach-Bahl, K., Gasche, R., Breuer, L., and Papen, H.: Fluxes of NO and N$_2$O from temperate forest soils: impact of
890 forest type, N deposition and of liming on the NO and N$_2$O emissions, Nutrient Cycling in Agroecosystems, 48, 79–90,
doi:10.1023/a:1009785521107, 1997.

Chaparro-Suarez, I., Meixner, F., and Kesselmeier, J.: Nitrogen dioxide (NO$_2$) uptake by vegetation controlled by atmospheric
concentrations and plant stomatal aperture, Atmospheric Environment, 45, 5742–5750, doi:10.1016/j.atmosenv.2011.07.021,
2011

895 Damgaard, C., Jensen, L., Frohn, L. M., Borchsenius, F., Nielsen, K. E., Ejrnæs, R. and Stevens, C. J.: The effect of nitrogen
deposition on the species richness of acid grasslands in Denmark: A comparison with a study performed on a European scale,
Environmental Pollution, 159, 1778-1782, doi:10.1016/j.envpol.2011.04.003, 2011.

Delaria, E. R., Vieira, M., Cremieux, J., and Cohen, R. C.: Measurements of NO and NO$_2$ exchange between the atmosphere
and Quercus agrifolia, Atmospheric Chemistry and Physics, 18, 14 161–14 173, doi:10.5194/acp-18-14161-2018, 2018.

900 Delaria, E. R., Place, B. K., Liu, A. X., and Cohen, R. C.: Laboratory measurements of stomatal NO$_2$ deposition to native
California trees and the role of forests in the NO$_x$ cycle, Atmospheric Chemistry and Physics, 20, 14 023–14 041,
doi:10.5194/acp-20-14023-2020, 2020.

de Vries, W., Reinds, G. J., and Vel, E.: Intensive monitoring of forest ecosystems in Europe: 2: Atmospheric deposition and
its impacts on soil solution chemistry, Forest Ecology and Management, 174, 97–115, doi:10.1016/S0378-1127(02)00030-0,
905 2003.

Dirnböck, T., Grandin, U., Bernhardt-Römermann, M., Beudert, B., Canullo, R., Forsius, M., Grabner, M.-T., Holmberg, M.,
Kleemola, S., Lundin, L., Mirtl, M. Neumann, M., Pompei, E., Salemaa, M., Starlinger, F., Staszewski, T., and Uziębło, A.
K.: Forest floor vegetation response to nitrogen deposition in Europe, Global Change Biology, 20, 429-440, doi:
10.1111/gcb.12440 , 2014.

910 Dirnböck, T., Pröll, G., Austnes, K., Beloica, J., Beudert, B., Canullo, R., De Marco, A., Fornasier, M. F., Futter, M., Goergen,
K., Grandin, U., Holmberg, M., Lindroos, A.-J., Mirtl, M., Neirynck, J., Pecka, T., Nieminen, T. M., Nordbakken, J.-F., Posch,
M., Reinds, G.-J., Rowe, E. C., Salemaa, M., Scheuschner, T., Starlinger, F., Uziębło, A. K., Valinia, S., Weldon, J., Wamelink,
W. G. W., and Forsius, M.: Currently legislated decreases in nitrogen deposition will yield only limited plant species recovery
in European forests, Environmental research letters, 13, 125010, doi: 10.1088/1748-9326/aaf26b, 2018.

915 Draaijers, G. P. J. and Erisman, J. W.: A canopy budget model to assess atmospheric deposition from throughfall
measurements, Water, Air, Soil Pollution, 85, 2253–2258, doi: 10.1007/BF01186169, 1995.

Emberson, L.D., Ashmore, M. R., Simpson, D., Tuovinen, J.-P. and Cambridge, H. M.: Towards a model of ozone deposition
and stomatal uptake over Europe, EMEP/MSC-W 6/2000, Norwegian Meteorological Institute, Oslo, 2000a.

Emberson, L. D., Ashmore, M. R., Cambridge, H. M., Simpson, D., and Tuovinen, J. P.: Modelling stomatal ozone flux across
920 Europe, Environmental Pollution, 109, 403–13, doi:10.1016/S0269-7491(00)00043-9, 2000b.

Erisman, J. W., Van Pul, A., and Wyers, P.: Parametrization of surface resistance for the quantification of atmospheric
deposition of acidifying pollutants and ozone, Atmospheric Environment, 28, 2595–2607, doi:10.1016/1352-2310(94)90433-
2, 1994.

Erisman, J. W., Galloway, J., Seitzinger, S., Bleeker, A. and Butterbach-Bahl, K.: Reactive nitrogen in the environment and
925 its effect on climate change, Current Opinion in Environmental Sustainability, 3, 281-290, doi:10.1016/j.cosust.2011.08.012.,
2011.

Erisman, J. W., Galloway, J. N., Seitzinger, S., Bleeker, A., Dise, N. B., Petrescu, A. M., Leach, A. M. and de Vries, W.:
Consequences of human modification of the global nitrogen cycle, Philosophical Transactions of the Royal Society London
B: Biological Sciences, 368, 20130116, doi: 10.1098/rstb.2013.0116, 2013.

930 Falge, E., Baldocchi, D., Olson, R., Anthoni, P., Aubinet, M., Bernhofer, C., Burba, G., Ceulemans, R., Clement, R., Dolman,
H., Granier, A., Gross, P., Grünwald, T., Hollinger, D., Jensen, N.-O., Katul, G., Keronen, P., Kowalski, A., Lai, C. T., Law,

B. E., Meyers, T., Moncrieff, J., Moors, E., Munger, J., Pilegaard, K., Üllar Rannik, Rebmann, C., Suyker, A., Tenhunen, J., Tu, K., Verma, S., Vesala, T., Wilson, K., and Wofsy, S.: Gap filling strategies for defensible annual sums of net ecosystem exchange, Agricultural and Forest Meteorology, 107, 43–69, doi:10.1016/S0168-1923(00)00225-2, 2001.

935 Farmer, D. K., Wooldridge, P. J., and Cohen, R. C.: Application of thermal-dissociation laser induced fluorescence (TD-LIF) to measurement of HNO_3, Σalkyl nitrates, Σperoxy nitrates, and NO_2 fluxes using eddy covariance, Atmospheric Chemistry and Physics, 6, 3471–3486, doi:10.5194/acp-6-3471-2006, 2006.

Farmer, D. K. and Cohen, R. C.: Observations of HNO_3, ΣAN, ΣPN and NO_2 fluxes: evidence for rapid HO_x chemistry within a pine forest canopy, Atmospheric Chemistry and Physics, 8, 3899–3917, doi:10.5194/acp-8-3899-2008, 2008.

940 Ferm, M.: A Sensitive Diffusional Sampler, Report L91-172, Swedish Environmental Research Institute, Gothenburg, 1991.

Ferrara, R. M., Loubet, B., Di Tommassi, P., Bertolini, T., Magliulo, V., Cellier, P., Eugster, W., and Rana, G.: Eddy covarinance measurement of ammonia fluxes: Comparison of high frequency correction methodologies, Agricultural and Forest Meteorology, 158-159, 30-42, doi:10.1016/j.agrformet.2012.02.001, 2012.

Ferrara, R. M., Di Tommassi, P., Farmulari, D., and Rana G.: Limitations of an Eddy-Covariance System in Measuring Low

945 Ammonia Fluxes, Boundary-Layer Meteorology, 180, 173-186, doi:10.1007/s10546-021-00612-6, 2021.

Finkelstein, P. L. and Sims, P. F.: Sampling error in eddy correlation flux measurements, Journal of Geophysical Research: Atmospheres, 106, 3503–3509, doi: 10.1029/2000JD900731, 2001.

Flechard, C. R., Nemitz, E., Smith, R. I., Fowler, D., Vermeulen, A. T., Bleeker, A., Erisman, J. W., Simpson, D., Zhang, L., Tang, Y. S., and Sutton, M. A.: Dry deposition of reactive nitrogen to European ecosystems: a comparison of inferential models

950 across the NitroEurope network, Atmos. Chem. Phys., 11, 2703–2728, doi:10.5194/acp-11-2703-2011, 2011.

Flechard, C. R., Ibrom, A., Skiba, U. M., de Vries, W., van Oijen, M., Cameron, D. R., Dise, N. B., Korhonen, J. F. J., Buchmann, N., Legout, A., Simpson, D., Sanz, M. J., Aubinet, M., Loustau, D., Montagnani, L., Neirynck, J., Janssens, I. A., Pihlatie, M., Kiese, R., Siemens, J., Francez, A.-J., Augustin, J., Varlagin, A., Olejnik, J., Juszczak, R., Aurela, M., Berveiller, D., Chojnicki, B. H., Dammgen, U., Delpierre, N., Djuricic, V., Drewer, J., Dufrene, E., Eugster, W., Fauvel, Y., Fowler, D.,

955 Frumau, A., Granier, A., Gross, P., Hamon, Y., Helfter, C., Hensen, A., Horvath, L., Kitzler, B., Kruijt, B., Kutsch, W. L., Lobo-do Vale, R., Lohila, A., Longdoz, B., Marek, M. V., Matteucci, G., Mitosinkova, M., Moreaux, V., Neftel, A., Ourcival, J.-M., Pilegaard, K., Pita, G., Sanz, F., Schjoerring, J. K., Sebastia, M.-T., Tang, Y. S., Uggerud, H., Urbaniak, M., van Dijk, N., Vesala, T., Vidic, S., Vincke, C., Weidinger, T., Zechmeister-Boltenstern, S., Butterbach-Bahl, K., Nemitz, E., and Sutton, M. A.: Carbon–nitrogen interactions in European forests and semi-natural vegetation – Part 1: Fluxes and budgets of carbon,

960 nitrogen and greenhouse gases from ecosystem monitoring and modelling, Biogeosciences, 17, 1583–1620, doi:10.5194/bg-17-1583-2020, 2020.

Fowler, D., Coyle, M., Skiba, U., Sutton, M. A., Cape, J. N., Reis, S., Sheppard, L. J., Jenkins, A., Grizzetti, B., Galloway, J. N., Vitousek, P., Leach, A., Bouwman, A. F., Butterbach-Bahl, K., Dentener, F., Stevenson, D., Amann, M. and Voss, M.: The global nitrogen cycle in the twenty-first century, Philosophical Transactions of the Royal Society B: Biological Sciences,

965 368, 20130164, doi: 10.1098/rstb.2013.0164, 2013.

Galloway, J. N., Aber, J. D., Erisman, J. W., Seitzinger, S. P., Howarth, R. W., Cowling, E. B. and Cosby, B. J.: The Nitrogen Cascade, BioScience, 53, 341-356, doi: 10.1641/0006-3568(2003)053[0341:TNC]2.0.CO;2, 2003.

Garland, J. A.: The Dry Deposition of Sulphur Dioxide to Land and Water Surfaces, Proceedings of the Royal Society A: Mathematical, Physical and Engineering Sciences, 354, 245–268, doi:10.1098/rspa.1977.0066, 1977.

970 Ge, X., Schaap, M., Kranenburg, R., Segers, A., Reinds, G. J., Kros, H., and de Vries, W.: Modeling atmospheric ammonia using agricultural emissions with improved spatial variability and temporal dynamics, Atmos. Chem. Phys., 20, 16055–16087, doi:10.5194/acp-20-16055-2020, 2020.

Geddes, J. A. and Murphy, J. G.: Observations of reactive nitrogen oxide fluxes by eddy covariance above two midlatitude North American mixed hardwood forests, Atmospheric Chemistry and Physics, 14, 2939–2957, doi:10.5194/acp-14-2939-2014, 2014.

975

Grandin, U.: Epiphytic algae and lichen cover in boreal forests - a long-term study along a N and S deposition gradient in Sweden, Ambio, 40, 8, 857-866, doi: 10.1007/s13280-011-0205-x, 2011.

Hansen, K., Sørensen, L. L., Hertel, O., Geels, C., Skjøth, C. A., Jensen, B., and Boegh, E.: Ammonia emissions from

980 deciduous forest after leaf fall, Biogeosciences, 10, 4577–4589, doi:10.5194/bg-10-4577-2013, 2013.

Hansen, K., Pryor, S. C., Boegh, E., Hornsby, K. E., Jensen, B., and Sørensen, L. L.: Background concentrations and fluxes of atmospheric ammonia over a deciduous forest, Agricultural and Forest Meteorology, 214-215, 380–392, doi: 10.1016/j.agrformet.2015.09.004, 2015.

Hettelingh, J.-P., Posch, M., De Smet, P. A. M. and Downing, R. J.: The use of critical loads in emission reduction agreements

985 in Europe, Water, Air, and Soil Pollution., 85, 2381-2385, doi:10.1007/BF01186190, 1995.

Hettelingh, J.-P., Posch, M., Velders, G. J. M., Ruyssenaars, P., Adams, M., de Leeuw, F., Lükewille, A., Maas, R., Sliggers, J. and Slootweg, J.: Assessing interim objectives for acidification, eutrophication and ground-level ozone of the EU National Emission Ceilings Directive with 2001 and 2012 knowledge, Atmospheric Environment, 75, 129-140, doi:10.1016/j.atmosenv.2013.03.060, 2013.

990 Horii, C. V., Munger, J. W., Wofsy, S. C., Zahniser, M., Nelson, D., and McManus, J. B.: Fluxes of nitrogen oxides over a temperate deciduous forest, Journal of Geophysical Research: Atmospheres, 109, doi:10.1029/2003JD004326, 2004.

Horii, C. V., Munger, J. W., Wofsy, S. C., Zahniser, M., Nelson, D., and McManus, J. B.: Atmospheric reactive nitrogen concentration and flux budgets at a Northeastern US forest site, Agricultural and Forest Meteorology, 136, 159–174, doi:10.1016/j.agrformet.2006.03.005, 2006.

995 Jarvis, P. G.: The Interpretation of the Variations in Leaf Water Potential and Stomatal Conductance Found in Canopies in the Field, Philos. T. R. Soc. B, 273, 593–610, doi:10.1098/rstb.1976.0035, 1976.

Jensen, N. and Hummelshøj, P.: Derivation of canopy resistance for water vapor fluxes over a spruce forest, using a new technique for the viscous sublayer resistance (correction to vol. 73, p. 339, 1995), Agricultural and Forest Meteorology, 85, 289, doi:10.1016/S0168-1923(97)00024-5, 1997.

1000 Jensen, N. O. and Hummelshøj, P.: Derivation of canopy resistance for water-vapor fluxes over a spruce forest, using a new technique for the viscous sublayer resistance, Agricultural and Forest Meteorology, 73, 339–352, doi:10.1016/0168-1923(94)05083-I, 1995.

Jung, H., Senf, C., Beudert, B., and Krueger, T.: Bayesian hierarchical modeling of nitrate concentration in a forest stream affected by large-scale forest dieback, Water Resources Research, 57, 2, e2020WR027264, doi: 10.1029/2020WR027264

1005 2021.

Krupa, S. V.: Effects of atmospheric ammonia (NH_3) on terrestrial vegetation: a review, Environmental Pollution, 124, 179-211, doi: 10.1016/S0269-7491(02)00434-7, 2003.

Kuenen, J., Dellaert, S., Visschedijk, A., Jalkanen, J.-P., Super, I., and Denier van der Gon, H.: CAMS-REG-v4: a state-of-the-art high-resolution European emission inventory for air quality modelling, Earth System Science Data, 14, 491–515, doi:

1010 10.5194/essd-14-491-2022, 2022.

Kundu, S., Kawamura, K., and Lee, M.: Seasonal variation of the concentrations of nitrogenous species and their nitrogen isotopic ratios in aerosols at Gosan, Jeju Island: Implications for atmospheric processing and source changes of aerosols, Journal of Geophysical Research: Atmospheres., 115, D20305, doi: 10.1029/2009JD013323, 2010.

Li, Y., Schichtel, B. A., Walker, J. T., Schwede, D. B., Chen, X., Lehman, C. M. B., Puchalski, M. A., Gay, D. A., and Collett, J. L.; Increasing importance of deposition of reduced nitrogen in the United States, Proceedings of the National Academy of Sciences, 113, 5874-5879, doi: 10.1073/pnas.1525736113, 2016.

Marx, O., Brümmer, C., Ammann, C., Wolff, V., and Freibauer, A.: TRANC – a novel fast-response converter to measure total reactive atmospheric nitrogen, Atmospheric Measurement Techniques, 5, 1045–1057, doi:10.5194/amt-5-1045-2012, 2012.

Manders-Groot, A. M. M., Segers, A. J., and Jonkers, S.: LOTOS-EUROS v2.0 Reference Guide, TNO report TNO2016 R10898, TNO, Utrecht, The Netherlands, https://lotos-euros.tno.nl/media/10360/reference_guide_v2-0_r10898.pdf (last access: 14 March 2022), 2016.

Manders, A. M. M., Builtjes, P. J. H., Curier, L., Denier van der Gon, H. A. C., Hendriks, C., Jonkers, S., Kranenburg, R., Kuenen, J. J. P.,Segers, A. J., Timmermans, R. M. A., Visschedijk, A. J. H., Wichink Kruit, R. J., van Pul, W. A. J., Sauter, F. J., van der Swaluw, E., Swart, D. P. J., Douros, J., Eskes, H., van Meijgaard, E., van Ulft, B., van Velthoven, P., Banzhaf, S., Mues, A. C., Stern, R., Fu, G., Lu, S., Heemink, A., van Velzen, N., and Schaap, M.: Curriculum vitae of the LOTOS–EUROS (v2.0) chemistry transport model, Geoscientific Model Development, 10, 4145–4173, doi:10.5194/gmd-10-4145-2017, 2017.

Milford, C., Hargreaves, K. J., Sutton, M. A., Loubet, B., and Cellier, P.: Fluxes of NH_3 and CO_2 over upland moorland in the vicinity of agricultural land, Journal of Geophysical Research: Atmospheres, 106, 24 169–24 181, doi:10.1029/2001jd900082, 2001.

Min, K.-E., Pusede, S. E., Browne, E. C., LaFranchi, B. W., Wooldridge, P. J., and Cohen, R. C.: Eddy covariance fluxes and vertical concentration gradient measurements of NO and NO_2 over a ponderosa pine ecosystem: observational evidence for within canopy chemical removal of NO_x, Atmospheric Chemistry and Physics, 14, 5495–5512, doi:10.5194/acp-14-5495-2014, 2014.

Moravek, A., Singh, S., Pattey, E., Pelletier, L., and Murphy, J. G.: Measurements and quality control of ammonia eddy covariance fluxes: A new strategy for high frequency attenuation correction, Atmospheric Measurement Techniques, 12, 6059–6078, doi:10.5194/amt-12-6059-2019, 2019.

Munger, J. W., Wofsy, S. C., Bakwin, P. S., Fan, S. M., Goulden, M. L., Daube, B. C., Goldstein, A. H., Moore, K. E., and Fitzjarrald, D. R.: Atmospheric deposition of reactive nitrogen oxides and ozone in a temperate deciduous forest and a subarctic woodland: 1. Measurements and mechanisms, Journal of Geophysical Research-Atmospheres, 101, 12 639–12 657, doi:10.1029/96JD00230, 1996.

Nemitz, E., Sutton, M. A., Wyers, G. P., and Jongejan, P. A. C.: Gas-particle interactions above a Dutch heathland: I. Surface exchange fluxes of NH_3, SO_2, HNO_3 and HCl, Atmospheric Chemistry and Physics, 4, 989–1005, doi:10.5194/acp-4-989-2004, 2004.

Paulissen, M.P.C.P., Bobbink, R., Robat, S.A., and Verhoeven, J. T. A.: Effects of Reduced and Oxidised Nitrogen on Rich-Fen Mosses: a 4-Year Field Experiment., Water, Air, & Soil Pollution, 227, 18, doi:10.1007/s11270-015-2713-y, 2016.

Paulson, C. A.: The Mathematical Representation of Wind Speed and Temperature Profiles in the Unstable Atmospheric Surface Layer, Journal of Applied Meteorology, 9, 857–861, doi:10.1175/1520-0450(1970)009<0857:Tmrows>2.0.Co;2, 1970.

Reichstein, M., Falge, E., Baldocchi, D., Papale, D., Aubinet, M., Berbigier, P., Bernhofer, C., Buchmann, N., Gilmanov, T., Granier, A., Grünwald, T., Havránková, K., Ilvesniemi, H., Janous, D., Knohl, A., Laurila, T., Lohila, A., Loustau, D., Matteucci, G., Meyers, T., Miglietta, F., Ourcival, J.-M., Pumpanen, J., Rambal, S., Rotenberg, E., Sanz, M., Tenhunen, J., Seufert, G., Vaccari, F., Vesala, T., Yakir, D., and Valentini, R.: On the separation of net ecosystem exchange into assimilation and ecosystem respiration: review and improved algorithm, Global Change Biology, 11, 1424–1439, doi:10.1111/j.1365-2486.2005.001002.x, 2005.

Putaud, J.-P., Van Dingenen, R., Alastuey, A., Bauer, H., Birmili, W., Cyrys, J., Flentje, H., Fuzzi, S., Gehrig, R., Hansson, H., Harrison, R., Herrmann, H., Hitzenberger, R., Hüglin, C., Jones, A., Kasper-Giebl, A., Kiss, G., Kousa, A., Kuhlbusch, T., Löschau, G., Maenhaut, W., Molnar, A., Moreno, T., Pekkanen, J., Perrino, C., Pitz, M., Puxbaum, H., Querol, X., Rodriguez, S., Salma, I., Schwarz, J., Smolik, J., Schneider, J., Spindler, G., ten Brink, H., Tursic, J., Viana, M., Wiedensohler, A., and Raes, F.: A European aerosol phenomenology – 3: Physical and chemical characteristics of particulate matter from 60 rural, urban, and kerbside sites across Europe, Atmospheric Environment, 44, 1308–1320, doi: 10.1016/j.atmosenv.2009.12.011, 2010.

Rosenkranz, P., Brüggemann, N., Papen, H., Xu, Z., Seufert, G., and Butterbach-Bahl, K.: N2O, NO and CH4 exchange, and microbial N turnover over a Mediterranean pine forest soil, Biogeosciences, 3, 121–133, doi: 10.5194/bg-3-121-2006, 2006.

Roth, M., Müller-Meißner, A., Michiels, H.-G., and Hauck, M.: Vegetation changes in the understory of nitrogen-sensitive temperate forests over the past 70 years, Forest Ecology and Management, 503, 119754, doi: 10.1016/j.foreco.2021.119754 2022.

Rummel, U., Ammann, C., Gut, A., Meixner, F. X., and Andreae, M. O.: Eddy covariance measurements of nitric oxide flux within an Amazonian rain forest, Journal of Geophysical Research-Atmospheres, 107, LBA 17–1–LBA 17–9, doi:10.1029/2001JD000520, 2002.

Sauter, F., Sterk, M., van der Swaluw, E., Wichink Kruit, R., de Vries, W., and van Pul, A.: The OPS-model: Description of OPS 5.0.0.0, RIVM, Bilthoven, https://www.rivm.nl/media/ops/OPS-model.pdf (last access: 14 March 2022), 2020.

Saylor, R. D., Baker, B. D., Lee, P., Tong, D., Pan, L., and Hicks, B. B.: The particle dry deposition component of total deposition from air quality models: right, wrong or uncertain?, Tellus B: Chemical and Physical Meteorology, 71, 1550324, doi: 10.1080/16000889.2018.1550324, 2019.

Schaap, M., Wichink Kruit, R., Hendriks, C., Kranenburg, R., Segers, A., Builtjes, P., and Banzhaf, S.: Modelling and assessment of acidifying and eutrophying atmospheric deposition to terrestrial ecosystems (PINETI-2): Part I: Atmospheric deposition to German natural and semi-natural ecosystems during 2009, 2010 and 2011, techinal report, Umweltbundesamt, Dessau-Roßlau, Germany, https://www.umweltbundesamt.de/sites/default/files/medien/1410/publikationen/2017-08-15_texte_62-2017_pineti2-teil1.pdf (last access: 14 March 2022), 2017.

Schaap. M., Hendriks, C., Kranenburg, R., Kuenen, J., Segers, A., Schlutow, A., Nagel, H.-D., Ritter, A., and Banzhaf, S.: PINETI-3: Modellierung atmosphärischer Stoffeinträge von 2000 bis 2015 zur Bewertung der ökosystem-spezifischen Gefährdung von Biodiversität durch Luftschadstoffe in Deutschland, technical report, Umweltbundesamt, Dessau-Roßlau, Germany, https://www.umweltbundesamt.de/sites/default/files/medien/1410/publikationen/2018-10-17_texte_79-2018_pineti3.pdf (last access: 14 March 2022), 2018.

Schneider, C., Pelzer, M., Toenges-Schuller, N., Nacken, M., & Niederau, A.: ArcGIS basierte Lösung zur detaillierten, deutschlandweiten Verteilung (Gridding) nationaler Emissionsjahreswerte auf Basis des Inventars zur Emissionsberichterstattung - Kurzfassung; UBA TEXTE 71/2016. Für Mensch & Umwelt, https://www.umweltbundesamt.de/publikationen/arcgis-basierte-loesung-zur-detaillierten (last access: 9 June 2022), 2016.

Schrader, F. and Brümmer, C.: Land Use Specific Ammonia Deposition Velocities: a Review of Recent Studies (2004–2013), Water, Air, and Soil Pollution, 225, 2114, doi:10.1007/s11270-014-2114-7, 2014.

Schrader, F., Brümmer, C., Flechard, C. R., Wichink Kruit, R. J., van Zanten, M. C., Zöll, U., Hensen, A., and Erisman, J. W.: Non-stomatal exchange in ammonia dry deposition models: comparison of two state-of-the-art approaches, Atmospheric Chemistry and Physics, 16, 13417–13430, doi:10.5194/acp-16-13417-2016, 2016.

Schrader, F., Schaap, M., Zöll, U., Kranenburg, R., and Brümmer, C.: The hidden cost of using low-resolution concentration data in the estimation of NH3 dry deposition fluxes, Scientific Reports, 8, 969, doi:10.1038/s41598-017-18021-6, 2018.

Schrader, F, Erisman, J. W., and Brümmer, C: Towards a coupled paradigm of NH3-CO2 biosphere–atmosphere exchange modelling. Global Change Biology, 26, 4654–4663, doi: 10.1111/gcb.15184, 2020.

Schwarz, J., Cusack, M., Karban, J., Chalupníčková, E., Havránek, V., Smolík, J., and Ždímal, V.: PM$_{2.5}$ chemical composition at a rural background site in Central Europe, including correlation and air mass back trajectory analysis, Atmospheric Research, 176–177, 108–120, doi: 10.1016/j.atmosres.2016.02.017, 2016.

Schwede, D., Zhang, L., Vet, R., and Lear, G.: An intercomparison of the deposition models used in the CASTNET and CAPMoN networks, Atmospheric Environment, 45, 1337–1346, doi: 10.1016/j.atmosenv.2010.11.050, 2011.

Staelens, J., Houle, D.and De Schrijver, A., Neirynck, J., and Verheyen, K.: Calculating Dry Deposition and Canopy Exchange with the Canopy Budget Model: Review of Assumptions and Application to Two Deciduous Forests, Water, Air, and Soil Pollution, 191, 149–169, doi:10.1007/s11270-008-9614-2, 2008.

Sutton, M. A. and Fowler, D.: A Model for Inferring Bi-directional Fluxes of Ammonia Over Plant Canopies, in: Proceedings of the WMO conference on the measurement and modelling of atmospheric composition changes including pollutant transport, pp. 179–182, WMO/GAW (Gobal Atmosphere Watch)-91, Geneva, Switzerland, 1993.

Sutton, M. A., Tang, Y. S., Miners, B., and Fowler, D.: A New Diffusion Denuder System for Long-Term, Regional Monitoring of Atmospheric Ammonia and Ammonium, Water, Air and Soil Pollution: Focus, 1, 145–156, doi:10.1023/a:1013138601753, 2001.

Sutton, M. A., Howard, C. M., Erisman, J. W., Billen, G., Bleeker, A., Grennfelt, P., van Grinsven, H. and Grizzetti, B.: The European Nitrogen Assessment: sources, effects and policy perspectives, Cambridge University Press, Cambridge, UK, 2011.

Sutton, M. A., Reis, S., Riddick, S. N., Dragosits, U., Nemitz, E., Theobald, M. R., Tang, Y. S., Braban, C. F. , Vieno, M., Dore, A. J., Mitchell, R. F., Wanless, S., Daunt, F., Fowler, D., Blackall, T. D., Milford, C., Flechard, C. R., Loubet, B., Massad, R., Cellier, P., Personne, E., Coheur, P. F., Clarisse, L. Van Damme, M., Ngadi, Y., Clerbaux, C., Skjoth, C. A., Geels, C., Hertel, O., Wichink Kruit, R. J., Pinder, R. W., Bash, J. O., Walker, J. T., Simpson, D., Horvath, L., Misselbrook, T. H., Bleeker, A., Dentener, F. and de Vries, W.: Towards a climate-dependent paradigm of ammonia emission and deposition, Philosophical Transactions of the Royal Society of London. Series B.: Biological Sciences, 368, 20130166, doi: 10.1098/rstb.2013.0166, 2013.

Tang, Y. S., Simmons, I., van Dijk, N., Di Marco, C., Nemitz, E., Dämmgen, U., Gilke, K., Djuricic, V., Vidic, S., Gliha, Z., Borovecki, D., Mitosinkova, M., Hanssen, J. E., Uggerud, T. H., Sanz, M. J., Sanz, P., Chorda, J. V., Flechard, C. R., Fauvel, Y., Ferm, M., Perrino, C., and Sutton, M. A.: European scale application of atmospheric reactive nitrogen measurements in a low-cost approach to infer dry deposition fluxes, Agriculture, Ecosystems and Environment, 133, 183–195, doi:10.1016/j.agee.2009.04.027, 2009.

Tang, Y. S., Cape, J. N., Braban, C. F., Twigg, M. M., Poskitt, J., Jones, M. R., Rowland, P., Bentley, P., Hockenhull, K., Woods, C., Leaver, D., Simmons, I., van Dijk, N., Nemitz, E., and Sutton, M. A.: Development of a new model DELTA sampler and assessment of potential sampling artefacts in the UKEAP AGANet DELTA system: summary and technical report, Tech. rep., London, available at: https://uk-air.defra.gov.uk/library/reports?report_id=861 (last access: 22 July 2022), 2015.

Tang, Y. S., Flechard, C. R., Dämmgen, U., Vidic, S., Djuricic, V., Mitosinkova, M., Uggerud, H. T., Sanz, M. J., Simmons, I., Dragosits, U., Nemitz, E., Twigg, M., van Dijk, N., Fauvel, Y., Sanz, F., Ferm, M., Perrino, C., Catrambone, M., Leaver, D., Braban, C. F., Cape, J. N., Heal, M. R., and Sutton, M. A.: Pan-European rural monitoring network shows dominance of NH$_3$ gas and NH$_4$NO$_3$ aerosol in inorganic atmospheric pollution load, Atmospheric Chemistry and Physics, 1, 875–914, doi: 10.5194/acp-21-875-2021, 2021.

Tarnay, L. W., Gertler, A., and Taylor, G. E.: The use of inferential models for estimating nitric acid vapor deposition to semi-arid conifer-ous forests, Atmospheric Environment, 36, 3277–3287, doi:10.1016/S1352-2310(02)00303-5, 2002.

Thoene, B., Rennenberg, H., and Weber, P.: Absorption of atmospheric NO$_2$ by spruce (Picea abies) trees, New Phytologist, 134, 257–266, doi:10.1111/j.1469-8137.1996.tb04630.x, 1996.

Ulrich, B.: Nutrient and acid-base budget of central european forest ecosystems, in: Effects of Acid Rain on Forest Processes, edited by: Godbold, D., and Hüttermann, A., John Wiley & Sons, New York, USA, 1–50, 1994.

Van der Graaf, S. C., Kranenburg, R., Segers, A. J., Schaap, M., and Erisman, J. W.: Satellite-derived leaf area index and roughness length information for surface–atmosphere exchange modelling: a case study for reactive nitrogen deposition in north-western Europe using LOTOS-EUROS v2.0, Geoscientific Model Development, 13, 2451–2474, doi:10.5194/gmd-13-2451-2020, 2020.

Van Jaarsveld, J. A.: The Operational Priority Substances model. Description and validation of OPS-Pro 4.1., RIVM, Bilthoven, report 500045001, https://www.pbl.nl/sites/default/files/downloads/500045001.pdf (last access: 14 March 2022), 2004.

Van Oss, R., Duyzer, J., and Wyers, P.: The influence of gas-to-particle conversion on measurements of ammonia exchange over forest, Atmospheric Environment, 32, 465 – 471, doi:10.1016/S1352-2310(97)00280-X, 1998.

Van Pul, W. A. J. and Jacobs, A. F. G.: The conductance of a maize crop and the underlying soil to ozone under various environmental conditions, Boundary-Layer Meteorology, 69, 83–99, doi:10.1007/BF00713296, 1994.

Van Zanten, M. C., Sauter, F. J., Wichink Kruit, R. J., van Jaarsveld, J. A., and van Pul, W. A. J.: Description of the DEPAC module; Dry deposition modeling with DEPAC_GCN2010, Tech. rep., RIVM, Bilthoven, NL, 2010.

VDI: VDI-Guideline 3782 Part 5: Environmental meteorology – Atmospheric dispersion models – Deposition parameters, Tech. rep., Verein Deutscher Ingenieure, Düsseldorf, DE, 2006.

Webb, E. K.: Profile relationships: The log-linear range, and extension to strong stability, Quarterly Journal of the Royal Meteorological Society, 96, 67–90, doi:10.1002/qj.49709640708, 1970.

Wentworth, G. R., Murphy, J. G., Benedict, K. B., Bangs, E. J., and Collett Jr, J. L.: The role of dew as a nighttime reservoir and morning source for atmospheric ammonia, Atmospheric Chemistry and Physics Discussions, 16, 1–36, doi:10.5194/acp-2016-169, 2016.

Whitehead, J. D., Twigg, M., Famulari, D., Nemitz, E., Sutton, M. A., Gallagher, M. W., and Fowler, D.: Evaluation of laser absorption spectroscopic techniques for eddy covariance flux measurements of ammonia, Environ Sci Technol, 42, 2041–6, doi:10.1021/es071596u, 2008.

Wichink Kruit, R. J., van Pul, W. A. J., Sauter, F. J., van den Broek, M., Nemitz, E., Sutton, M. A., Krol, M., and Holtslag, A. A. M.: Modeling the surface–atmosphere exchange of ammonia, Atmospheric Environment, 44, 945–957, doi:10.1016/j.atmosenv.2009.11.049, 2010.

Wichink Kruit, R. J., Schaap, M., Sauter, F. J., van Zanten, M. C., and van Pul, W. A. J.: Modeling the distribution of ammonia across Europe including bi-directional surface–atmosphere exchange, Biogeosciences, 9, 5261–5277, doi:10.5194/bg-9-5261-2012, 2012.

Wichink Kruit, R. J., Aben, J., de Vries, W., Sauter, 1180F., van der Swaluw, E., van Zanten, M. C., and van Pul, W. A. J.: Modelling trends in ammonia in the Netherlands over the period 1990–2014, Atmospheric Environment, 154, 20–30, doi: 10.1016/j.atmosenv.2017.01.031, 2017.

Wintjen, P., Ammann, C., Schrader, F., and Brümmer, C.: Correcting high-frequency losses of reactive nitrogen flux measurements, Atmospheric Measurement Techniques, 13, 2923–2948, doi:10.5194/amt-13-2923-2020, 2020.

Wintjen, P., Schrader, F., Schaap, M., Beudert, B., and Brümmer, C.: Forest–atmosphere exchange of reactive nitrogen in a remote region – Part I: Measuring temporal dynamics, Biogeosciences, 19, 389–413, doi:10.5194/bg-19-389-2022, 2022.

Wyers, G. and Duyzer, J.: Micrometeorological measurement of the dry deposition flux of sulphate and nitrate aerosols to coniferous forest, Atmospheric Environment, 31, 333 – 343, doi:10.1016/S1352-2310(96)00188-4, 1997.

Wyers, G. P. and Erisman, J. W.: Ammonia exchange over coniferous forest, Atmospheric Environment, 32, 441–451, doi:10.1016/S1352-2310(97)00275-6, 1998.

Zhang, L., Gong, S., Padro, J., and Barrie, L.: A size-segregated particle dry deposition scheme for an atmospheric aerosol module, Atmospheric Environment, 35, 549-560, doi:10.1016/S1352-2310(00)00326-5, 2001.

1185 Zöll, U., Brümmer, C., Schrader, F., Ammann, C., Ibrom, A., Flechard, C. R., Nelson, D. D., Zahniser, M., and Kutsch, W. L.: Surface–atmosphere exchange of ammonia over peatland using QCL-based eddy-covariance measurements and inferential modeling, Atmospheric Chemistry and Physics, 16, 11 283–11 299, doi:10.5194/acp-16-11283-2016, 2016.

Zöll, U., Lucas-Moffat, A. M., Wintjen, P., Schrader, F., Beudert, B., and Brümmer, C.: Is the biosphere-atmosphere exchange of total reactive nitrogen above forest driven by the same factors as carbon dioxide? An analysis using artificial neural

1190 networks, Atmospheric Environment, 206, 108–118, doi: 10.1016/j.atmosenv.2019.02.042, 2019.